

# Tailless/TLX reverts intermediate neural progenitors to stem cells driving tumourigenesis via repression of *asense*/ASCL1

Anna E Hakes, Andrea H Brand\*

The Gurdon Institute and Department of Physiology, Development and Neuroscience, University of Cambridge, Cambridge, United Kingdom

**Abstract** Understanding the sequence of events leading to cancer relies in large part upon identifying the tumour cell of origin. Glioblastoma is the most malignant brain cancer but the early stages of disease progression remain elusive. Neural lineages have been implicated as cells of origin, as have glia. Interestingly, high levels of the neural stem cell regulator TLX correlate with poor patient prognosis. Here we show that high levels of the *Drosophila* TLX homologue, Tailless, initiate tumourigenesis by reverting intermediate neural progenitors to a stem cell state. Strikingly, we could block tumour formation completely by re-expressing *Asense* (homologue of human ASCL1), which we show is a direct target of Tailless. Our results predict that expression of TLX and ASCL1 should be mutually exclusive in glioblastoma, which was verified in single-cell RNA-seq of human glioblastoma samples. Counteracting high TLX is a potential therapeutic strategy for suppressing tumours originating from intermediate progenitor cells.

## Introduction

The underlying mechanisms of glioblastoma initiation and growth have proved challenging to elucidate. This is due, in part, to the extensive molecular heterogeneity of glioblastoma, both between patients and within individual tumours. As such, there are many potential routes to tumourigenesis and the cell fate changes that contribute to glioblastoma initiation and progression remain to be fully elucidated. Cell fates can be altered in many different ways during tumourigenesis, depending upon the combination of genetic mutations present and the tumour cell of origin.

Mouse models have revealed many of the different cell types that can give rise to glioblastoma. In the central nervous system (CNS), tumours have been induced experimentally from differentiated glial cells, glial precursors and neural stem/progenitor cells (Alcantara Llaguno *et al.*, 2015; Alcantara Llaguno *et al.*, 2009; Bachoo *et al.*, 2002; Chow *et al.*, 2011; Friedmann-Morvinski *et al.*, 2012; Holland *et al.*, 2000; Lindberg *et al.*, 2009; Marumoto *et al.*, 2009). A recent study revealed that astrocyte-like neural stem cells (NSCs) in the SVZ of glioblastoma patients harbour driver mutations that are found in the patient's tumour, suggesting that astrocyte-like NSCs are cells of origin of glioblastoma in humans (Lee *et al.*, 2018). Neural lineages become more resistant to glioblastoma transformation as differentiation progresses, supporting stem cells or early progenitor cells as a common source of glioblastoma (Alcantara Llaguno *et al.*, 2019). However, it is difficult to state unequivocally which cell type gives rise to tumours in mouse models of glioblastoma due in part to the lack of specific markers and driver lines. For example, both stem and progenitor cells express Nestin (Chen *et al.*, 2009) and GFAP labels both stem cells and astrocytes (Doetsch *et al.*, 1999). Furthermore, the mechanism through which cells within NSC lineages change identity during tumourigenesis and contribute to tumour aggressiveness remains unclear.

\*For correspondence:  
a.brand@gurdon.cam.ac.uk

**Competing interests:** The authors declare that no competing interests exist.

**Funding:** See page 16

**Received:** 06 November 2019

**Accepted:** 19 February 2020

**Published:** 19 February 2020

**Reviewing editor:** Claude Desplan, New York University, United States

© Copyright Hakes and Brand. This article is distributed under the terms of the [Creative Commons Attribution License](#), which permits unrestricted use and redistribution provided that the original author and source are credited.

The *Drosophila* CNS has proved extremely valuable for understanding the fundamental principles of cancer (Deng, 2019; Villegas, 2019). The availability of an unparalleled *Drosophila* genetic toolkit and extensive knowledge of neural cell fate transitions has enabled diverse aspects of tumorigenesis to be investigated. One *Drosophila* model of glioblastoma is based on co-activation of EGFR and PI3K in glial cells (Chen and Read, 2019; Chen et al., 2019; Chen et al., 2018; Read et al., 2009; Read et al., 2013; Witte et al., 2009). This model recapitulates some of the features of glioblastoma, however, co-activation of EGFR and PI3K does not transform NSCs or their progeny. As a result the model does not address the contribution of neural lineages to glioblastoma (Read et al., 2009).

High levels of the orphan nuclear receptor TLX (also known as NR2E1, Nuclear Receptor Subfamily 2 Group E Member 1) have been observed in glioblastoma and been shown to correlate with poor patient prognosis (Park et al., 2010; Zou et al., 2012). TLX is expressed in adult NSCs, where it is required for neurogenesis in both the subventricular zone (SVZ) and the subgranular zone (SGZ) (Liu et al., 2008; Liu et al., 2010; Shi et al., 2004; Zhang et al., 2008; Zou et al., 2012). TLX is also expressed in glioblastoma stem cells (Zhu et al., 2014) and upregulation of TLX promotes gliomagenesis in the mouse SVZ (Liu et al., 2010). These results indicate that TLX is an important stem cell regulator both in normal and tumorigenic conditions. However, it is not known how abnormally high TLX levels affect the identity of cells in NSC lineages nor has the cell type vulnerable to TLX overexpression been identified.

In *Drosophila*, different NSC lineages exhibit distinct vulnerabilities to tumour-inducing mutations (Hakes and Brand, 2019). The majority of lineages arise from Type I NSCs (Figure 1A) that divide asymmetrically to self-renew and generate ganglion mother cells (GMCs), which then undergo terminal division (Figure 1B; Harding and White, 2018; Ramon-Cañellas et al., 2019). A much smaller number of Type II NSCs, by contrast, generate intermediate neural progenitors (INPs) (Figure 1B'; Bello et al., 2008; Boone and Doe, 2008; Bowman et al., 2008) that are themselves able to self-renew and produce GMCs. These transit amplifying Type II lineages more closely resemble neural lineages in the vertebrate CNS and provide an opportunity to investigate whether conserved mechanisms regulate how NSCs and their progeny respond to tumorigenic insults.

Here we show that the *Drosophila* TLX homologue, Tailless (Tll), is required to direct the identity of Type II NSCs during development. We found that high levels of Tll are sufficient to initiate tumours from differentiating Type II NSC lineages by directing a cell fate change from INP to NSC. To identify downstream effectors of Tll action, we mapped the genome-wide targets of Tll and identified the proneural gene *asense* as a direct target of Tll repression, both during development and in tumorigenesis. Strikingly, we were able to rescue Tll tumours completely, and restore normal neurogenesis, by re-expressing *asense*. Our results demonstrate a reciprocal relationship between Tll and *Asense* expression and we hypothesized that this relationship might hold true in glioblastoma. We found that expression of TLX and ASCL1 (human counterparts of Tll and *Asense*) are also mutually exclusive in glioblastoma, suggesting a potentially conserved route to tumorigenesis.

## Results

### Tailless is necessary for Type II NSC identity and lineage progression

To understand the role Tailless (Tll) plays in the development of Type II NSC lineages, we first assessed its expression pattern. We found that Tll was expressed in Type II NSCs throughout larval development (Figure 1—figure supplement 1A–C). We detected *tll* mRNA in Type II NSCs but not in their progeny (INPs) (Figure 1C), while Tll protein was present in NSCs and at low levels in newly-born INPs (Figure 1D–D'). Tll shares a high degree of homology with human TLX (Figure 1E; Jackson et al., 1998): their DNA binding domains are 81% identical (94% similarity) and their ligand binding domains are 40% identical (77% similarity). In addition, TLX and Tll bind to the same consensus DNA sequence (Yu et al., 1994) and recruit conserved cofactors, such as Atrophin, via their ligand binding domains (Wang et al., 2006; Zhi et al., 2015). TLX is expressed in the neurogenic regions of the adult mouse brain (Liu et al., 2008; Niu et al., 2011; Shi et al., 2004; Zhang et al., 2008). In the SVZ, TLX is detected in NSCs and their progeny, intermediate progenitor cells (Figure 1F; Li et al., 2012; Obernier et al., 2011), which is very similar to the expression pattern of Tll in *Drosophila* Type II lineages (Figure 1G).

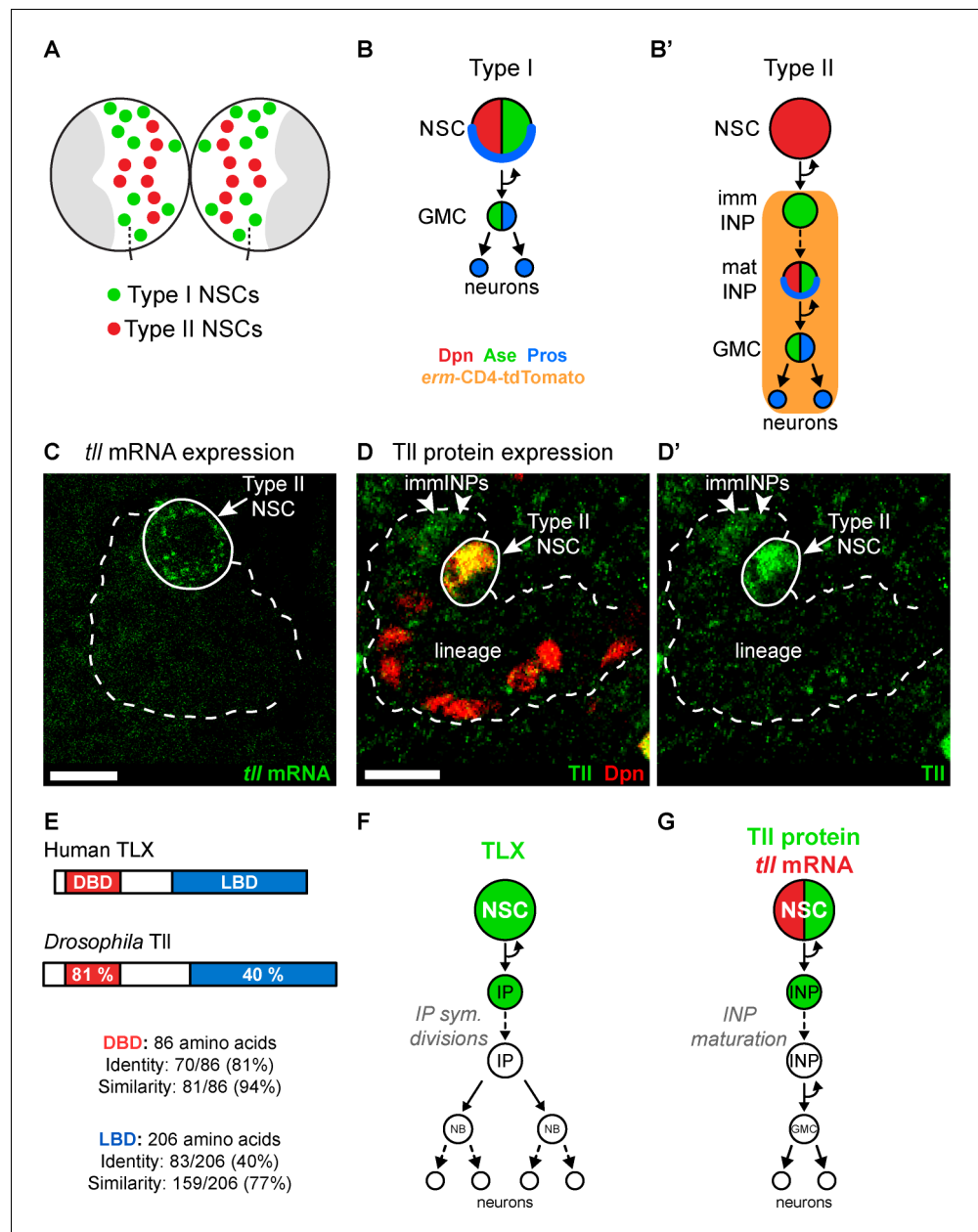


**Figure 1.** TII is expressed in *Drosophila* Type II NSCs. (A) Schematic showing the position of the eight Type II NSCs (red) in each brain lobe. The majority of stem cells in the *Drosophila* brain are Type I NSCs (green). The optic lobes, which generate the adult visual processing centre, are shown in grey. (B–B') Schematics showing the expression of cell fate markers in (B) Type I and (B') Type II lineages. NSC: neural stem cell; imm INP: immature intermediate neural progenitor; mat INP: mature intermediate neural progenitor; GMC: ganglion mother cell. (C) RNA FISH shows *tll* mRNA (green) expression in Type II NSCs (solid outline) but not in their lineages (dotted outline). Type II lineages were identified by *pntP1-GAL4 > mCD8-GFP* expression in the central brain at wandering third instar larval stage. (D–D') Immunostaining for TII (green) shows strong expression in Type II NSCs ( $Dpn^+$  (red), solid outline) and weak expression in  $Dpn^-$  immature INPs (immINPs, arrow heads). Mature INPs (small  $Dpn^+$  cells in the lineage) do not express TII. Type II lineages were identified by *pntP1-GAL4 > mCD8-GFP* expression in the central brain at wandering third instar larval stage. (E) Amino acid conservation between human TLX and *Drosophila* TII. (F) Schematic showing that TLX (green) is expressed in NSCs and intermediate progenitors (IPs) in SVZ of the adult mouse brain (Li et al., 2012; Obernier et al., 2011). (G) Schematic showing *tll* mRNA (red) and TII protein (green) expression in *Drosophila* Type II NSC lineages. Single section confocal images. Scale bars represent 10  $\mu$ m.

The online version of this article includes the following figure supplement(s) for figure 1:

Figure 1 continued on next page

Figure 1 continued

**Figure supplement 1.** Tll is expressed in *Drosophila* Type II NSCs.

The enrichment of Tll expression in Type II NSCs suggested a role for Tll in regulating Type II NSC identity or proliferation. We knocked down Tll in larval NSCs using *wor*-GAL4 using two independent RNAi constructs that target different regions of the *tll* coding sequence (**Figure 2—figure supplement 1A**). We scored expression of Deadpan (Dpn), a Hes family bHLH-O transcription factor that is expressed in all NSCs (*Bier et al., 1992*), and Asense (Ase), a proneural bHLH factor expressed in Type I but not Type II NSCs (*Bowman et al., 2008*). Expressing either *tll* RNAi construct resulted in the absence of all Type II NSC in all brains assessed (i.e. all NSCs expressed Dpn and Ase) (**Figure 2—figure supplement 1B–C**). We also generated *tll* null MARCM (Mosaic Analysis with a Repressible Cell Marker) clones (*Lee and Luo, 1999*). We found that Type II lineages were often labelled in wild type clones (**Figure 2—figure supplement 1D–D'**), demonstrating that MARCM clones could encompass Type II NSCs. However, we were unable to recover *tll* null Type II NSC clones, despite mutant clones being visible in other NSC lineages (**Figure 2—figure supplement 1E**). This suggested that *tll* null Type II NSCs underwent a cell fate transition that resulted in the loss of Type II markers. In support of this, quantification of the number of Type II lineages in brains with *tll* null clones revealed a reduction in the number of Type II lineages (**Figure 2—figure supplement 1F**). Furthermore, the number of absent Type II lineages in brains with *tll* null clones was comparable to the number of Type II lineages encompassed in MARCM clones in control brains (**Figure 2—figure supplement 1F**).

Next, we knocked down Tll expression specifically in Type II lineages by driving *tll* RNAi (*tll*-miRNA[s]), which effectively knocked down Tll protein (**Figure 2—figure supplement 1G**) with *pntP1*-GAL4 (*Zhu et al., 2011*) in combination with a 'FLP-out' GAL4 cassette to immortalise GAL4 expression (**Figure 2—figure supplement 2A**) and followed alterations in cell fate. While Dpn expression was unaffected, *tll* knockdown resulted in derepression of Ase in all Type II NSCs (**Figure 2—figure supplement 2B**), suggesting a switch in mode of neurogenesis from Type II to Type I.

To test whether Type II NSCs were transformed into Type I NSCs, we assessed lineage composition and gene expression. Type I NSCs express Dpn and Ase and segregate cortically localised Prospero (Pros) to their daughter cells (GMCs). In GMCs, Ase is expressed and Pros, a pro-differentiation transcription factor, translocates to the nucleus. In contrast, Type II NSCs express Dpn but not Ase or Pros. Type II NSCs give rise to INPs, which express Dpn, Ase and cortical Pros. INPs then generate GMCs that are Ase<sup>+</sup> Pros<sup>+</sup>. In addition, the Ets transcription factor PointedP1 (PntP1) is expressed in Type II NSCs and immature INPs but not in Type I lineages (*Zhu et al., 2011*). Type II lineages can also be labelled by expression driven by a regulatory fragment of the FezF transcription factor *earmuff* (*erm*), which is expressed from INPs onwards (*Pfeiffer et al., 2008; Weng et al., 2010*) but not in Type I lineages.

Strikingly, upon *tll* knockdown, no INPs (small Dpn<sup>+</sup> Ase<sup>+</sup>) could be found in Type II lineages and instead GMCs (Ase<sup>+</sup> Pros<sup>+</sup>) were positioned adjacent to the NSCs (compare **Figure 2A–A'** to **Figure 2B–B'**). In 6 out of 10 *tll* knockdown brains, at least one Type II NSC expressed Pros that localised in a crescent at the cell cortex, indicating asymmetric segregation of Pros to daughter cells (**Figure 2B'**). Asymmetric segregation of Pros is a feature characteristic of Type I NSCs and INPs that is never observed in Type II NSCs (*Bayraktar et al., 2010; Bello et al., 2008*). Furthermore, expression of Pnt-GFP (*Boisclair Lachance et al., 2014*) in Type II NSCs (**Figure 2—figure supplement 2C–C'**) and the Type II lineage marker, *erm*-CD4-tdTomato (*Han et al., 2011*), was lost in the absence of *tll* (**Figure 2—figure supplement 2D**). We conclude that, in the absence of *tll*, Type II NSC lineages are transformed into Type I lineages which exhibit lower neurogenic capacity due to the lack of INPs (**Figure 2C–C'** and **Figure 2—figure supplement 2E–E'**).

### Tailless tumours can arise from Type II INPs and Type I NSCs

We have shown that Type II NSCs are lost when Tll is downregulated. As a corollary, we hypothesised that ectopic expression of Tll might result in excess Type II NSCs. To test this, we drove Tll expression in INPs and their progeny with *erm*-GAL4 (*Pfeiffer et al., 2008; Weng et al., 2010*) in combination with a 'FLP-out' GAL4 cassette to immortalise GAL4 expression (*Ito et al., 1997*;



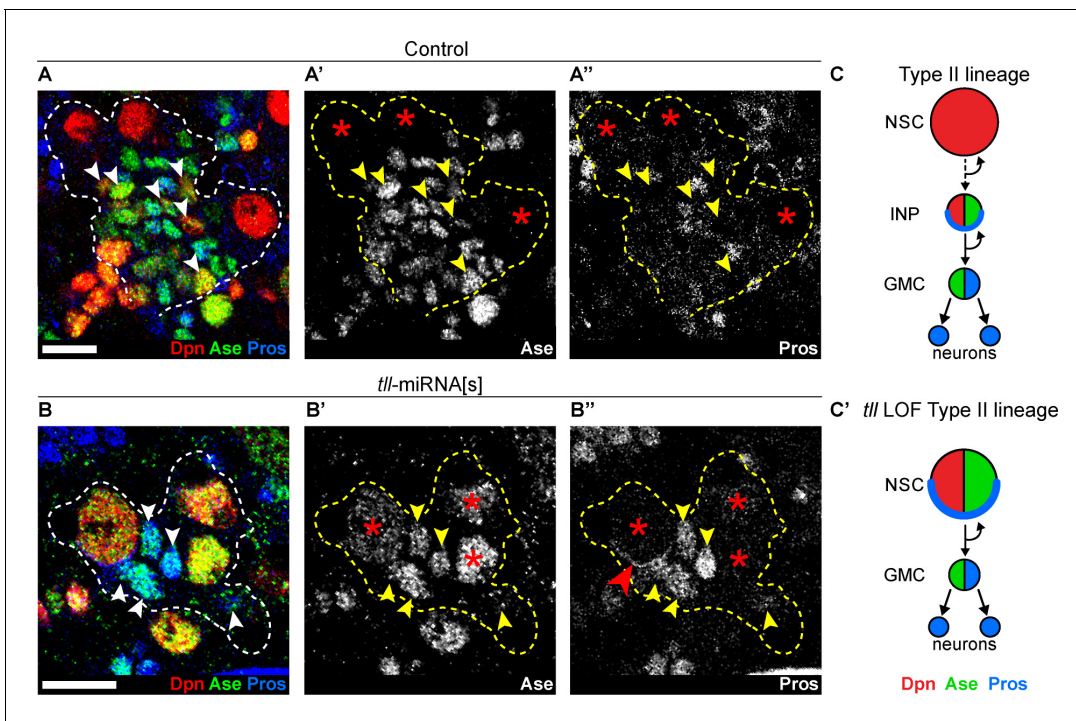


**Figure 2.** Tll is required for Type II NSC fate and lineage progression. (A–A'') Control Type II NSCs (Dpn<sup>+</sup> (red) and Ase<sup>-</sup> (green)) generate INPs (arrowheads, Dpn<sup>+</sup>, Ase<sup>+</sup> and Pros<sup>-</sup> (blue)). Dotted lines outline three Type II lineages. Red asterisks (\*) indicate Type II NSCs. *n* = 10 brains, dissected at the end of second larval instar stage. (B–B'') Upon *tll* knockdown using *pntP1 >act-GAL4* to drive UAS-*tll*-miRNA[s], Type II NSCs express Ase and generate GMCs directly (arrowheads, Ase<sup>+</sup> and Pros<sup>+</sup>) and exhibit Pros crescents (red arrowhead). Dotted lines outline three Type II lineages identified by *pntP1 >act-GAL4* driving UAS-*GFP*. Red asterisks (\*) indicate Type II NSCs. *n* = 10 brains, dissected at the end of second larval instar stage. (C–C') Schematic summarising the *tll* loss of function (LOF) phenotype in Type II NSCs. Single section confocal images. Scale bars represent 10 μm. The online version of this article includes the following figure supplement(s) for figure 2:

**Figure supplement 1.** Tll loss of function in Type II NSCs.

**Figure supplement 2.** Generating an immortalised Type II NSC driver to assess cell fate changes.

**Figure 3A** and **Figure 3—figure supplement 1A–B**). In control brain lobes there are only eight Type II NSCs. Tll misexpression in INPs resulted in a dramatic increase in the number of Type II NSCs, from 8 to  $109 \pm 12.12$  per brain lobe (**Figure 3B–B'** and quantified in **Figure 3C**). We also observed a strong reduction in the number of differentiating progeny in Type II lineages (**Figure 3—figure supplement 1C–D'**). We tested whether Tll expression in more differentiated neural precursors (GMCs) or post-mitotic neurons would also generate excess NSCs but, interestingly, we found that both cell types were resistant to ectopic Tll expression: we observed neither additional NSCs nor neuronal dedifferentiation (**Figure 3D–E'**). Therefore, ectopic Tll expression in Type II lineages promotes NSC fate at the expense of self-renewing cells, specifically INPs (**Figure 3—figure supplement 1E–E'**).

INPs closely resemble Type I NSCs, in that they divide in the same manner and express common cell fate markers (Dpn, Ase and cortical Pros; **Figure 1B–B'**). We tested if Type I NSCs, which are found throughout the CNS, are also vulnerable to high levels of Tll expression. When we expressed Tll throughout the CNS, we observed large tumour-like growths in the adult brain that consisted almost entirely of NSCs (Dpn<sup>+</sup> cells) (compare **Figure 4A–A'**). At larval stages, we found that high levels of Tll resulted in Dpn<sup>+</sup> NSCs in both the central brain and ventral nerve cord, indicating that ectopic Tll can induce tumours from Type I NSCs (**Figure 4B–B'**).

Expression of Tll in Type I NSCs (normally Tll<sup>-</sup>, Ase<sup>+</sup>) might convert them to a Type II fate (Tll<sup>+</sup>, Ase<sup>-</sup>). To determine if tumour initiation occurred via conversion of Type I to Type II NSCs, we assessed the expression of Ase in tumours in the ventral nerve cord, which normally contains only Type I NSCs. Remarkably, Tll-induced tumours consisted almost entirely of NSCs that were negative for Ase, indicating a Type II-like NSC fate (**Figure 4C–C'**). Consistent with a change in identity to

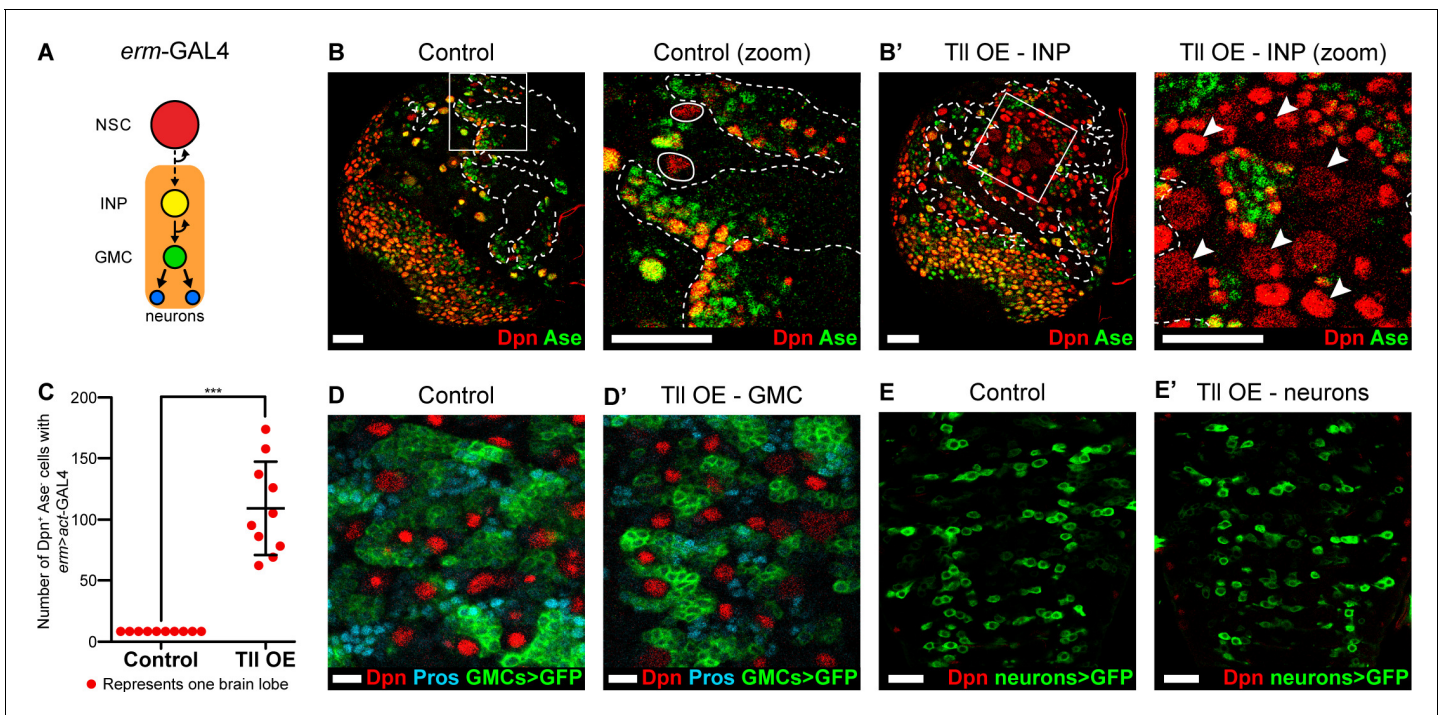


**Figure 3.** TII overexpression in INPs generates ectopic NSCs. (A) Schematic showing the expression of *erm*-GAL4, which begins to be expressed in Type II lineages during the final stages of INP maturation. (B–B') In Control (zoom), solid white outlines indicate Type II NSCs and *erm >act-GAL4* is expressed in their lineages (dotted white lines). TII OE in INPs with *erm >act-GAL4* resulted in a large expansion of Type II NSCs (Dpn<sup>+</sup> (red) and Ase<sup>-</sup> (green)) in Type II lineages. Arrowheads in TII OE – INP (zoom) highlight ectopic Type II NSCs. Zoom panels are magnifications of boxed regions in Control and TII overexpression (OE) – INP.  $n = 10$  brain lobes for Control and TII. UAS-*tll* expression was restricted to larval stages with *tub*-GAL80<sup>ts</sup> and brains were dissected at wandering third instar larval stage. (C) Quantification of the total number of Type II NSCs (Dpn<sup>+</sup> Ase<sup>-</sup>) in Control or TII OE *erm >act-GAL4* brains. Kolmogorov-Smirnov test \*\*\*,  $p < 0.001$  ( $p = 0.000091$ ). (D–D') Expressing TII in GMCs (using GMR71C09-GAL4 > *mCD8-GFP* (green)) does not result in ectopic NSCs (i.e. no Dpn<sup>+</sup> GFP<sup>+</sup> cells) nor defects in differentiation, as assessed by Pros (blue) staining.  $n = 10$  brains for Control,  $n = 12$  brains for TII OE. Brains were dissected at wandering third instar larval stage. (E–E') Expressing TII in neurons using OK371-GAL4 > *mCD8-GFP* (green) does not result in ectopic NSCs (i.e. no Dpn<sup>+</sup> GFP<sup>+</sup> cells).  $n = 4$  brains for Control and TII. Brains were dissected at wandering third instar larval stage. Single section confocal images. Scale bars represent 30  $\mu\text{m}$  in (B, B', E, E') and 10  $\mu\text{m}$  in (D, D'). The online version of this article includes the following figure supplement(s) for figure 3:

**Figure supplement 1.** TII overexpression in INPs results in ectopic Type II NSCs.

Type II NSC, the tumour NSCs lacked Pros (Figure 4D–D'; Bayraktar et al., 2010). Furthermore, a subset of these transformed Type I NSCs generated INPs (Figure 4—figure supplement 1A–A'), indicating that TII is sufficient to induce a switch in NSC identity. Interestingly, the absence of Pros from TII-induced hyperplasia had been reported previously (Kurusu et al., 2009) but had not been linked to a transformation from Type I to Type II NSC fate, or the ectopic appearance of INPs in the ventral nerve cord.

The appearance of the ectopic Type II-like NSCs (Dpn<sup>+</sup> Ase<sup>-</sup>) was associated with a reduction in GMCs and neurons, as assessed by expression of Pros (Figure 4D–D'). We conclude that expressing TII in Type I lineages not only directs a change in NSC identity but also blocks differentiation in these newly transformed lineages, resulting in large NSC tumours comprised of Type II NSCs (Figure 4E–E').

### TLX/Tailless tumour initiation occurs via the reversion of INPs to NSC fate

To determine the cell of origin of TII-induced tumours, we used G-TRACE (GAL4 technique for real-time and clonal expression) (Evans et al., 2009) to follow cell fate transformations within the Type II lineage. G-TRACE reports both current and historic GAL4 expression and so can be used to follow cell lineages (Figure 5—figure supplement 1A). *erm*-GAL4 driving G-TRACE labels INPs, but not

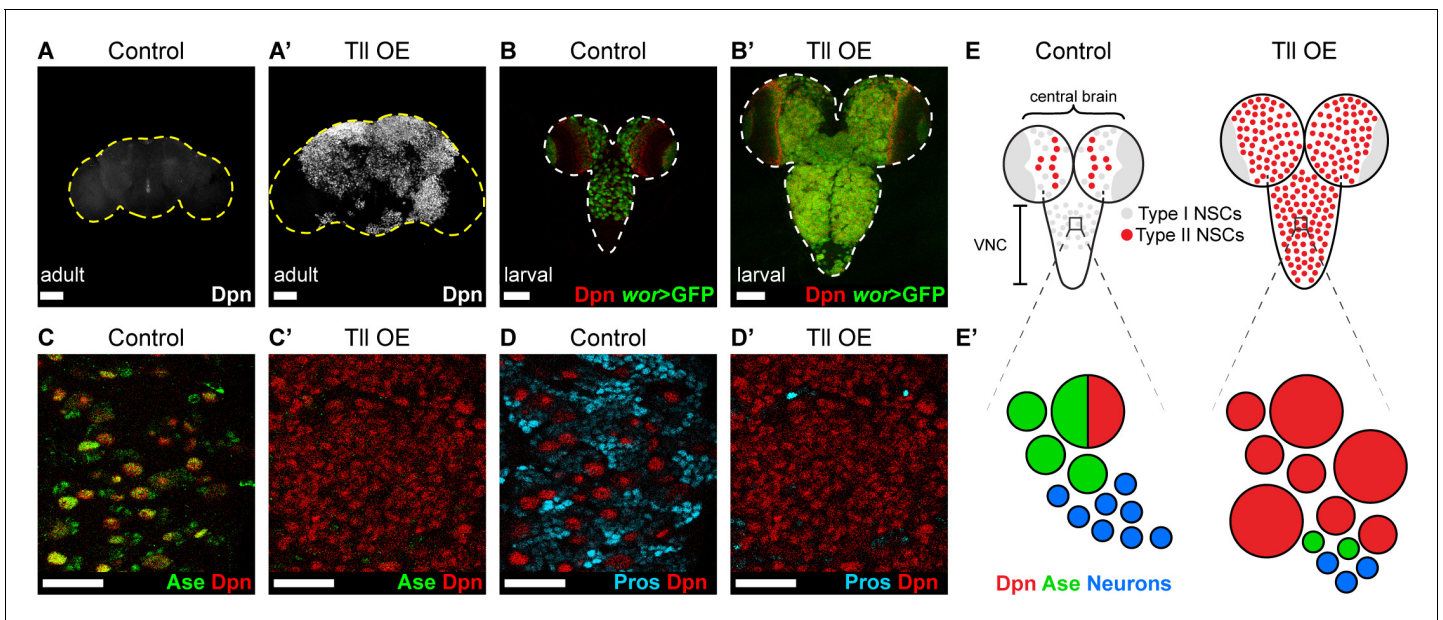


**Figure 4.** TII can initiate Type II NSC tumours from Type I NSCs. (A–A') Overexpression of *Drosophila* TII in neural lineages using *wor*-GAL4 resulted in NSC tumours (Dpn<sup>+</sup> (white)) in all adult brains assessed. Control adult brains did not contain any NSCs.  $n = 7$  brains for Control and TII OE. *UAS-tll* expression was restricted to late larval stages with *tub*-GAL80<sup>ts</sup> and brains were dissected from newly-eclosed adult flies. Images are projections over 15  $\mu$ m (Control) or 17  $\mu$ m (TII). (B–B') Overexpression of TII during larval development with *wor*-GAL4 resulted in large tumours consisting of ectopic NSCs (Dpn<sup>+</sup> (red) and *wor*-GAL4 > *mCD8-GFP* (green)) in the central brain and VNC of all brains assessed. *UAS-tll* expression was restricted to larval stages with *tub*-GAL80<sup>ts</sup> and brains were dissected at wandering third instar larval stage. (C–C') NSCs in the VNC are Type I (Dpn<sup>+</sup> (red) and *Ase*<sup>+</sup> (green)) in Control brains. TII-induced tumours (ectopic Dpn<sup>+</sup> cells) derived from Type I NSCs in the VNC are negative for *Ase*. *UAS-tll* expression was restricted to larval stages with *tub*-GAL80<sup>ts</sup> and brains were dissected at wandering third instar larval stage. (D–D') TII tumours in the VNC occur at the expense of differentiating progeny (*Pros* (blue)). *UAS-tll* expression was restricted to larval stages with *tub*-GAL80<sup>ts</sup> and brains were dissected at wandering third instar larval stage. (E) Schematic showing the organisation of Type I NSCs (*Ase*<sup>+</sup> (grey)) and Type II NSCs (*Ase*<sup>-</sup> (red)) in Control brains and TII OE brains. Note that in Control brains the VNC contains only Type I NSCs, whereas TII OE VNCs contain many ectopic Type II NSCs. (E') Schematic showing transformation of Type I NSC lineages in the VNC to ectopic Type II NSCs when TII is expressed at high levels. Single section confocal images unless stated otherwise. Scale bars represent 100  $\mu$ m in (A–B') and 30  $\mu$ m in (C–D').  $n = 10$  brains for all conditions unless stated otherwise.

The online version of this article includes the following figure supplement(s) for figure 4:

**Figure supplement 1.** TII is sufficient to induce the generation of INPs from a subset of Type I NSCs.

Type II NSCs, in control brains (Figure 5A). Expressing high levels of TII in INPs resulted in supernumerary Type II NSCs, which had previously expressed *erm*-GAL4 but lacked current expression (Figure 5A' and quantified in Figure 5B). This would be expected if the cells had originally been INPs (*erm*-GAL4 expressing) and were then transformed into Type II NSCs (*erm*-GAL4 negative). We conclude that TII expression is sufficient to induce a cell fate change from INP to NSC and our results implicate INP reversion to NSCs as the mechanism of tumour initiation.

To investigate whether human TLX could also initiate tumours from INPs via similar regulatory pathways, we expressed TLX in combination with G-TRACE in INPs. As for TII, we observed ectopic Type II NSCs with historic *erm*-GAL4 expression only (Figure 5A'). Our results indicate that both TII and TLX can initiate tumorigenesis from neural lineages by reverting INPs to NSCs (Figure 5C). Interestingly, neither TLX nor TII could revert post-mitotic neurons to NSCs, demonstrating that neurons are resistant to tumour initiation (see Figure 3D and Figure 5—figure supplement 2). We conclude that INPs represent a tumour-susceptible cell type and are the tumour cells of origin for TLX- and TII-induced tumours in *Drosophila* (Figure 5D).



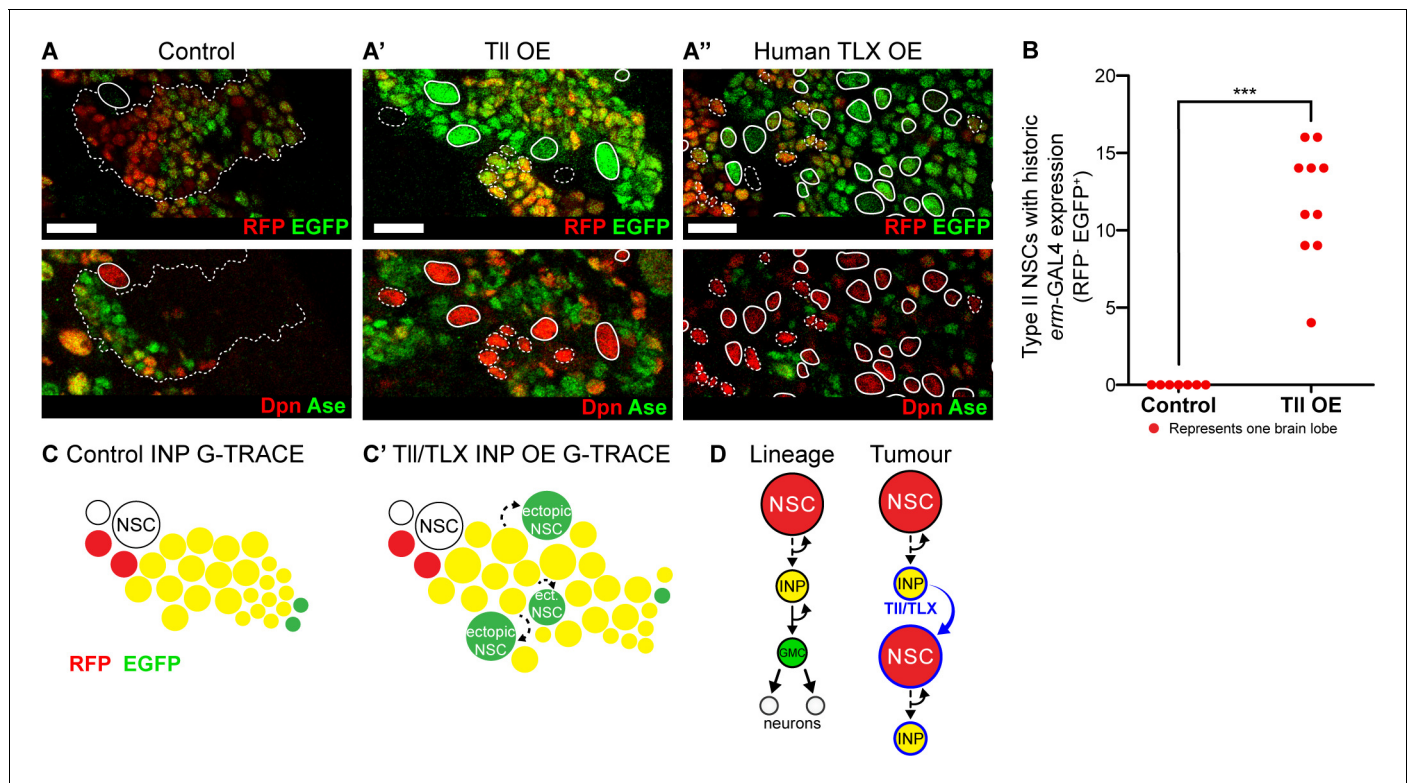


**Figure 5.** TII/TLX overexpression results in reversion of INPs to NSC fate. (A–A'') G-TRACE reveals current (RFP (red)) and historic (EGFP (green)) *erm-GAL4* expression (top panels). Dpn (red) and Ase (green) were used to assess the reversion of INPs to Type II NSCs (bottom panels). (A) In Control Type II lineages, NSCs (Dpn<sup>+</sup> Ase<sup>-</sup>, solid outline) are negative for both components of G-TRACE, whereas lineages show transition from RFP to EGFP (dotted outline). Overexpression (OE) of (A') TII or (A'') human TLX in INPs resulted in ectopic Type II NSCs (Dpn<sup>+</sup> Ase<sup>-</sup>, white outlines) that express the EGFP component of the G-TRACE only (solid outline). Dpn<sup>+</sup> Ase<sup>-</sup> NSCs with dotted white outline either express neither G-TRACE component (as in Control) or express both RFP and GFP (indicating current expression of *erm-GAL4*).  $n = 8$  brain lobes for Control and  $n = 10$  for TII and human TLX. Brains were dissected at wandering third instar stage. (B) Quantification of Type II NSCs expressing G-TRACE memory only (i.e. Dpn<sup>+</sup> Ase<sup>-</sup> and RFP<sup>+</sup> EGFP<sup>+</sup>). Kolmogorov-Smirnov test \*\*\*,  $p < 0.001$  ( $p = 0.000103$ ).  $n = 7$  brain lobes for Control;  $n = 10$  brain lobes for TII overexpression (OE). Brains were dissected at wandering third instar larval stage. (C–C') Schematic showing the expression of G-TRACE with the INP-specific *erm-GAL4* in Control brains or with TII/TLX OE. (D) A model for how TII/TLX generates ectopic NSCs and, consequently, tumours from INPs. Single section confocal images. Scale bars represent 15  $\mu\text{m}$ .

The online version of this article includes the following figure supplement(s) for figure 5:

**Figure supplement 1.** TII/TLX overexpression induces reversion of INPs to NSC fate.

**Figure supplement 2.** Expressing TLX in post-mitotic neurons does not result in ectopic NSCs.

## Ase restores progenitor identity and enforces differentiation to block Tailless tumours

We have shown that TII is both necessary and sufficient to repress *Ase* expression during development and in tumourigenesis. To investigate if TII represses *ase* directly, we identified the genome-wide TII binding sites in vivo using Targeted DamID (TaDa) (Southall et al., 2013). We profiled TII binding in Type II NSCs (16 per brain; approximately 700 NSCs per replicate) (Figure 6—figure supplement 1A–B) and identified TII-binding peaks at 2495 protein-coding genes (see 'TII TaDa binding targets.xlsx' for full list of TII targets), including *ase* (Figure 6—figure supplement 1C). We conclude that TII binds *ase* directly and represses its expression to promote Type II NSC fate. However, the loss of *Ase* alone is not sufficient to induce Type II fate in Type I NSCs (Bowman et al., 2008), indicating that TII acts on additional target genes to mediate this cell fate change and tumour initiation. One potential candidate is *Pros*, which we found was also bound by TII in Type II NSCs (Figure 6—figure supplement 1D). *Pros* is known to negatively regulate NSC proliferation (Cabernard and



*Doe, 2009*) and is also repressed when Tll is expressed at high levels (**Figure 3—figure supplement 1C–C'** and **Figure 4D–D'**; *Kurusu et al., 2009*).

As ectopic expression of Tll results in repression of *ase* and tumour formation, we investigated whether reinstating *ase* expression might be sufficient to block Tll-induced tumourigenesis. We expressed *Ase* together with Tll and found, remarkably, that tumourigenesis was completely abolished in all brains analysed ( $n = 10$ ) (**Figure 6A–A'**). Strikingly, not only did *Ase* prevent the production of ectopic NSCs, it also re-established normal neurogenesis in Type I NSC lineages: the

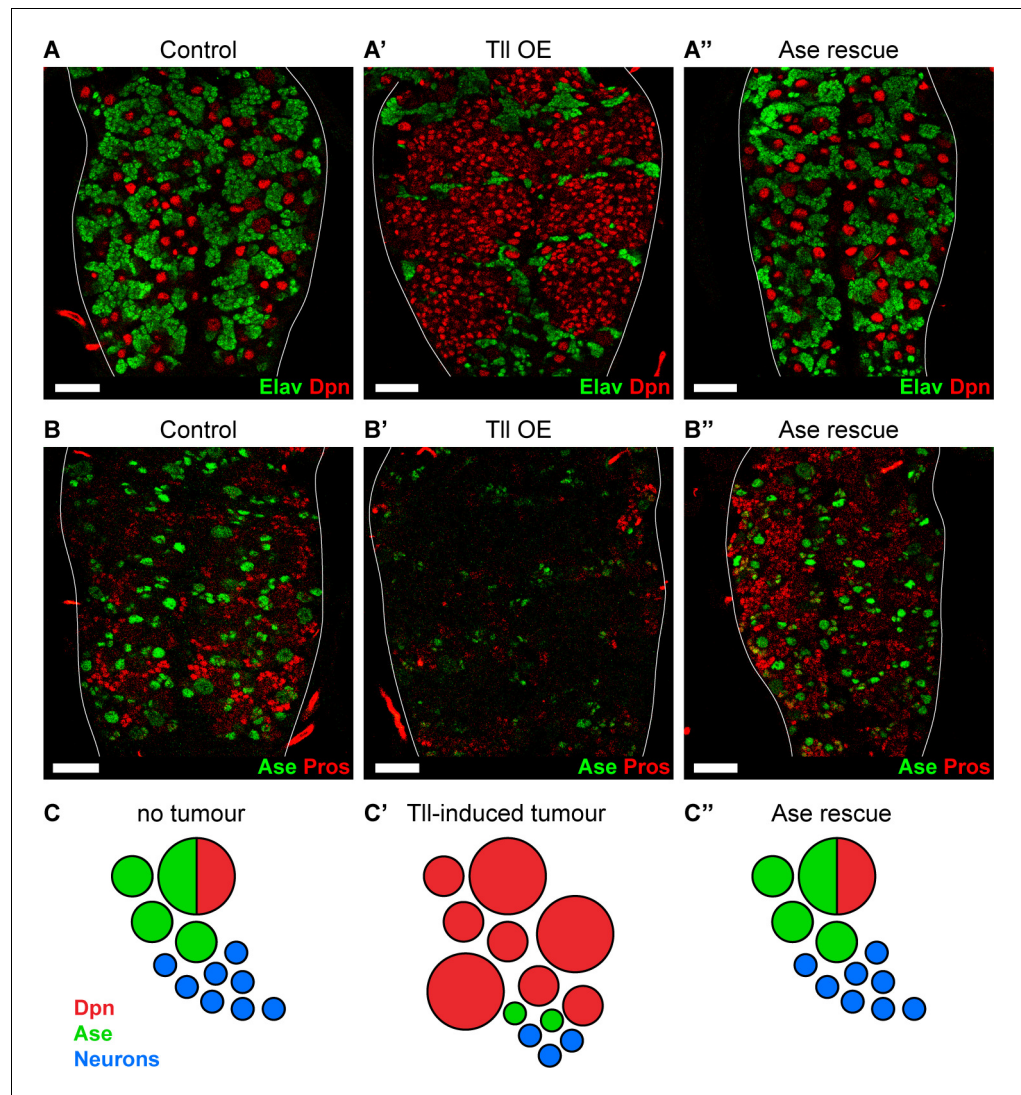


**Figure 6.** Reinstating progenitor identity prevents the formation of Tll tumours. (**A–A'**) Expressing *Ase* in combination with Tll during larval development using *wor*-GAL4 prevents tumour formation (ectopic *Dpn*<sup>+</sup> cells (red)) and restores neuronal differentiation (*Elav* (green)) in all brains assessed.  $n = 10$  brains for all conditions. Brains were dissected at wandering third instar stage. (**B–B'**) *Ase* (green) rescues Tll tumours by promoting differentiation (*Pros* (red)).  $n = 9$  brains for Control;  $n = 10$  brains for Tll overexpression (Tll OE) and *Ase* rescue. Brains were dissected at wandering third instar larval stage. (**C–C'**) Schematic depicting Type I NSC lineages (**C**) during development, (**C'**) with Tll-induced tumours and (**C''**) with *Ase* expression in Tll tumours. Single section confocal images. Scale bars represent 30  $\mu$ m.

The online version of this article includes the following source data and figure supplement(s) for figure 6:

**Figure supplement 1.** Determining Tll target genes in Type II NSCs using targeted DamID (TaDa).

**Figure supplement 2.** Ectopic *Ase* expression does not repress Tll.

**Figure supplement 2—source data 1.** Tll TaDa binding targets.

production of GMCs and neurons was restored, as revealed by expression of Pros and Elav (**Figure 6A–A'' and B–B''**). However, re-introducing Ase into Tll tumours did not repress the expression of Tll (**Figure 6—figure supplement 2A–A''**) nor does the ectopic expression of Ase turn off Tll in Type II NSCs (**Figure 6—figure supplement 2B–B'**). Therefore, by expressing Ase we were able to reinstate the normal neurogenic programme and prevent tumour initiation by Tll (**Figure 6C–C''**).

### TLX and ASCL1 appear to be mutually exclusive in human glioblastoma

We showed that, in *Drosophila*, Tll represses Ase both during development and in tumourigenesis. In other words, high levels of Tll correspond to low levels of Ase.

In human glioblastoma, high TLX expression is correlated with poor patient prognosis (**Park et al., 2010; Zou et al., 2012**). Intriguingly, ASCL1 levels also vary between human glioblastoma samples and low levels are correlated with shorter survival time (**Park et al., 2017**). Increasing ASCL1 levels was shown to promote terminal differentiation and attenuate tumorigenicity. Based on our results, we would predict that glioblastoma cells with high levels of TLX would exhibit low ASCL1 expression.

To determine if TLX and ASCL1 expression are mutually exclusive in glioblastoma, we analysed a previously published single-cell RNA sequencing (scRNA seq) data set that profiled glioblastoma samples from 28 patients, including both adult and pediatric tumours (**Nefitel et al., 2019**). Our analysis identified 7,835 single cells in this data set and, following cluster annotation based on previously known markers (**Nefitel et al., 2019**), we found that expression of both TLX and ASCL1 was restricted to the malignant glioblastoma cells (6,766 cells) (**Figure 7A–A'**). However, when we compared TLX and ASCL1 expression within the malignant population, we found very few cells that expressed both transcripts (**Figure 7B**), suggesting that TLX and ASCL1 are indeed mutually exclusive in malignant glioblastoma cells.

## Discussion

Our results revealed the mechanism through which high levels of the orphan nuclear receptor Tll initiate tumours in the *Drosophila* CNS (**Figure 8A**). We showed that Tll is expressed in Type II NSCs during larval development, where it is required for Type II NSC identity and subsequent lineage progression. In the absence of Tll, the proneural transcription factor Ase is derepressed in Type II NSCs. As a consequence, transit amplifying INPs are no longer generated and the resulting NSC lineages have a lower neurogenic potential.

A recent study examined the role of Tll in embryonic brain and showed that *tll* mutant embryos lack Type II NSCs (**Curt et al., 2019**). However, it was shown many years ago that *tll* mutant embryos fail to generate many NCSs, not just Type II NSCs, due to lack of *l'sc* expression that precedes NSC delamination (**Younossi-Hartenstein et al., 1997**). As a result, *tll* null mutants are not viable and the effect of *tll* loss of function on Type II NSCs specifically has not been addressed.

In mice, TLX is expressed in NSCs during embryonic development and in adulthood (**Li et al., 2012; Li et al., 2008; Liu et al., 2008; Shi et al., 2004**). Embryonic NSCs display defects in proliferation in the absence of TLX (**Li et al., 2008**) and the loss of TLX in adults results in the loss of transit-amplifying intermediates and reduction in neurogenesis (**Li et al., 2012; Liu et al., 2008; Niu et al., 2011; Shi et al., 2004**). While these effects were previously attributed to changes in the NSC cell cycle, our results suggest a cell fate change may occur due to the loss of TLX.

High levels of TLX in human glioblastoma are correlated with tumour aggressiveness (**Park et al., 2010; Zou et al., 2012**). High level expression of TLX results in glioblastoma-like lesions derived from SVZ NSC lineages in mouse models of glioblastoma (**Liu et al., 2010**) indicating that TLX can also promote glioblastoma development. However, it was not known how high TLX leads to glioblastoma, nor had the cellular origin of TLX-induced tumours been identified. TLX and its *Drosophila* homologue, Tll, are highly conserved proteins (**Yu et al., 1994**) and we found that both genes are able to revert INPs to NSC fate as a first step in tumour initiation. Ectopic expression of Tll was also sufficient to induce the expansion of NSCs throughout the *Drosophila* CNS, demonstrating the widespread vulnerability of NSC and progenitor populations to ectopic Tll expression.

We found that the ectopic NSCs resulting from high Tll expression are negative for Ase. We showed that Tll binds to the *ase* locus, suggesting that Tll directly represses *ase*. The absence of Ase

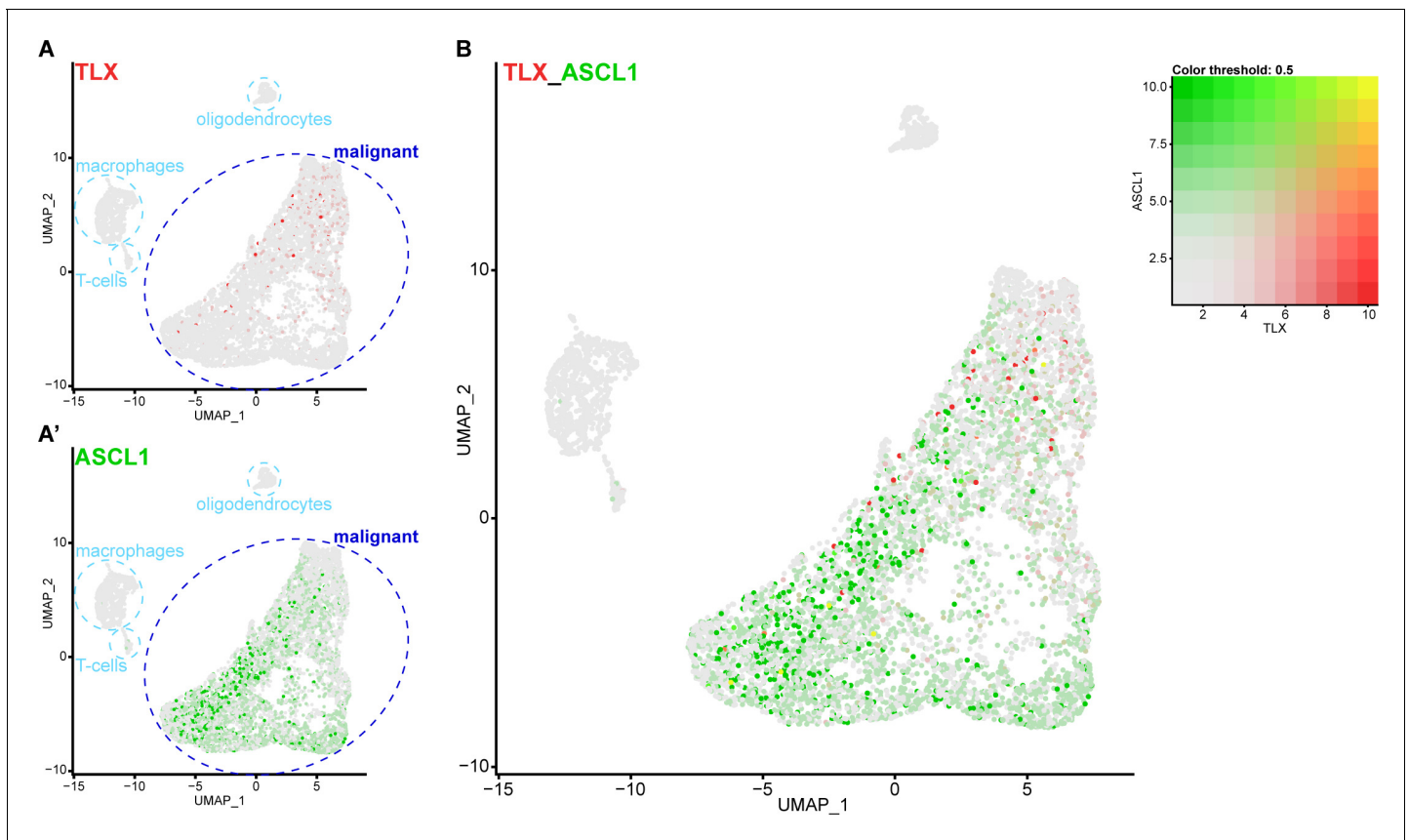


**Figure 7.** Single cell RNA sequencing reveals that TLX and ASCL1 appear to be mutually exclusive in human glioblastoma. (A) Uniform Manifold Approximation and Projection (UMAP) plot of 7,835 single cells coloured by TLX expression (red). Clusters were annotated based on previously known markers. TLX expression is only detected in the malignant cells. (A') UMAP plot coloured by ASCL1 expression (green). ASCL1 expression is only detected in the malignant cells. (B) UMAP plot coloured by expression of both TLX (red) and ASCL1 (green), which appear mutually exclusive. Yellow indicates cells that express high levels of both TLX and ASCL1. Single cell RNA sequencing data and cluster markers obtained from *Neftef et al. (2019)*.

is a hallmark of Type II NSCs. Therefore, ectopic Tll promotes a cell fate change from INP/Type I NSC to Type II NSC and thereby initiates tumourigenesis.

The capacity of Tll to induce NSC expansion had been reported previously as part of a study showing that Tll regulates the proliferation of larval mushroom body NSCs and GMCs (*Kurusu et al., 2009*). The authors showed that overexpressing Tll resulted in ectopic NSCs, but they did not identify the origin of these tumours and argued against a role for Tll in Type II NSC fate (*Kurusu et al., 2009*). Tll-induced tumourigenesis could be blocked by ectopic expression of Pros (*Kurusu et al., 2009*). However, ectopic Pros results in the loss of NSCs even in wild type brains (*Cabernard and Doe, 2009*). In contrast, Type I NSC lineages appear normal after Ase misexpression in wild type brains (*Bowman et al., 2008*). Furthermore, it has been reported that high levels of the human homologue of Pros, PROX1, exacerbate glioblastoma (*Elsir et al., 2010; Goudarzi et al., 2018; Roodakker et al., 2016; Xu et al., 2017*), arguing against PROX1 expression as a therapeutic strategy.

We found that the tumourigenic capacity of *Drosophila* Tll and human TLX was highly conserved (*Figure 8B*). Human TLX could also induce ectopic Type II NSCs from INPs through the repression of Ase. Analysis of scRNA seq from glioblastoma revealed that TLX and ASCL1 expression is mutually exclusive. It is notable that the origin of human glioblastoma has been mapped to the SVZ (*Lee et al., 2018*). While TLX positive NSCs have been identified in both the SVZ and dentate gyrus, high levels of TLX giving rise to glioblastoma has only been shown robustly in the SVZ (*Liu et al., 2010*). Furthermore, a recent study demonstrated that low expression levels of ASCL1 correlate with glioblastoma malignancy (*Park et al., 2017*). Ectopic expression of ASCL1 in glioblastoma stem cells

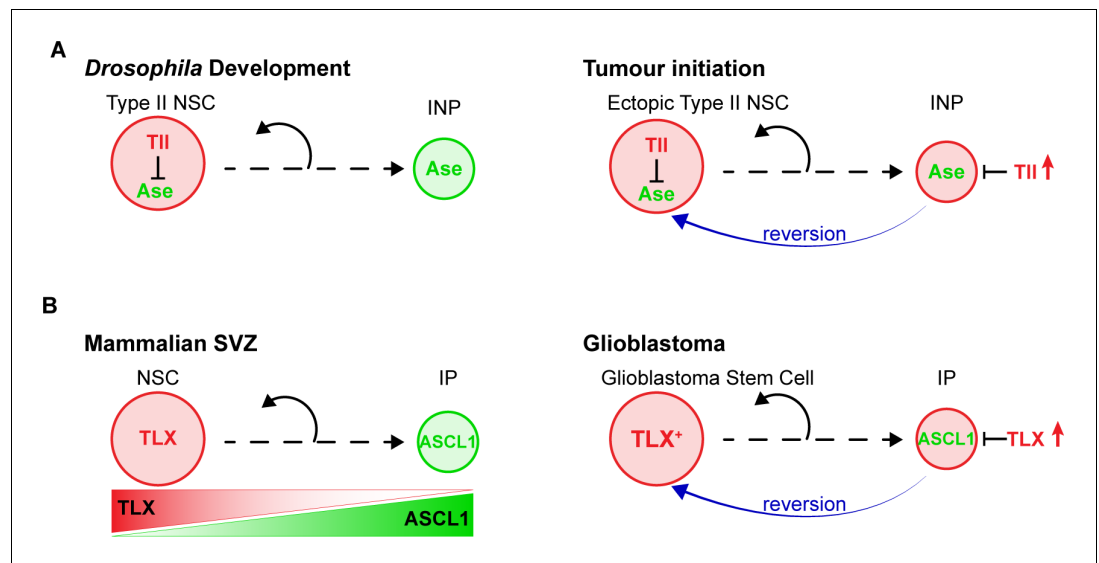


**Figure 8.** Model – TII reverts INPs to NSC fate to initiate tumourigenesis. (A) Schematics depicting the promotion of Type II NSC fate by TII (red) in development and tumourigenesis. TII must be down regulated in Type II lineages to allow differentiation. Ase (green) expression is activated during differentiation. If TII is high in INPs, or in Type I lineages, Type II NSC fate is maintained, or induced, and tumours form. (B) In the adult mouse SVZ, TLX expression is high in NSCs and lower in intermediate progenitors (IPs) (Li et al., 2012; Obernier et al., 2011), whereas ASCL1 is high in IPs and low in NSCs (Kim et al., 2011; Parras et al., 2004). Based on our results, we predict that high levels of TLX associated with aggressive glioblastoma revert IPs through the repression of ASCL1 to promote the generation of glioblastoma stem cells.

was sufficient to promote neuronal differentiation. Based on our results in *Drosophila*, we predict that introducing ASCL1 would override the repressive effect of TLX, induce neuronal differentiation and reduce tumour growth, thereby providing an effective treatment.

Our results indicate that INPs are the tumour initiating cells in Type II NSC lineages expressing high levels of the orphan nuclear receptor TII and potentially implicate intermediate progenitors as one of the cells of origin in TLX<sup>+</sup> glioblastomas, an aggressive and lethal brain tumour. We found that Ase is a direct target of TII and that Ase expression not only blocks TII-induced tumourigenesis, but also reinstates a normal neural differentiation programme.

## Materials and methods

### Key resources table

Reagent type (species) or resource	Designation	Source or reference	Identifiers	Additional information
Genetic reagent ( <i>D. melanogaster</i> )	w <sup>1118</sup> ;+;+	BDSC	RRID:BDSC_3605	
Genetic reagent ( <i>D. melanogaster</i> )	Ay-GAL4, UAS-GFP	BDSC	RRID:BDSC_4411	
Genetic reagent ( <i>D. melanogaster</i> )	Ay-GAL4, UAS-lacZ(nls)	BDSC	RRID:BDSC_4410	
Genetic reagent ( <i>D. melanogaster</i> )	btd-GAL4	(Estella et al., 2003)		
Genetic reagent ( <i>D. melanogaster</i> )	erm-GAL4	BDSC	RRID:BDSC_40731	GMR9D11-GAL4
Genetic reagent ( <i>D. melanogaster</i> )	GMR71C09-GAL4	BDSC	RRID:BDSC_39575	

Continued on next page



Continued

Reagent type (species) or resource	Designation	Source or reference	Identifiers	Additional information
Genetic reagent ( <i>D. melanogaster</i> )	insc-GAL4	(Luo et al., 1994)		GAL4 <sup>MZ1407</sup>
Genetic reagent ( <i>D. melanogaster</i> )	pntP1 <sup>14-94</sup> -GAL4	(Zhu et al., 2011)		
Genetic reagent ( <i>D. melanogaster</i> )	wor-GAL4	(Albertson et al., 2004)		
Genetic reagent ( <i>D. melanogaster</i> )	OK371-GAL4	BDSC	RRID:BDSC_26160	VGlut <sup>OK371</sup>
Genetic reagent ( <i>D. melanogaster</i> )	tub-GAL80 <sup>ts</sup>	BDSC	RRID:BDSC_7018	
Genetic reagent ( <i>D. melanogaster</i> )	UAS-ase	(Brand et al., 1993)		
Genetic reagent ( <i>D. melanogaster</i> )	UAS-FLP	BDSC	RRID:BDSC_4539	
Genetic reagent ( <i>D. melanogaster</i> )	UAS-FLP	BDSC	RRID:BDSC_4540	
Genetic reagent ( <i>D. melanogaster</i> )	UAS-lacZ	(Brand and Perrimon, 1993)		
Genetic reagent ( <i>D. melanogaster</i> )	UAS-LT3-NDam	(Southall et al., 2013)		
Genetic reagent ( <i>D. melanogaster</i> )	UAS-LT3-NDam-tII	this study		TII-Dam fusion for Targeted DamID
Genetic reagent ( <i>D. melanogaster</i> )	UAS-mCD8-GFP	BDSC	RRID:BDSC_5130	
Genetic reagent ( <i>D. melanogaster</i> )	UAS-mCD8-GFP	BDSC	RRID:BDSC_5137	
Genetic reagent ( <i>D. melanogaster</i> )	UAS-mCD8-mCherry	BDSC	RRID:BDSC_27391	
Genetic reagent ( <i>D. melanogaster</i> )	UAS-myr-mRFP	BDSC	RRID:BDSC_7118	
Genetic reagent ( <i>D. melanogaster</i> )	UAS-myr-mRFP	BDSC	RRID:BDSC_7119	
Genetic reagent ( <i>D. melanogaster</i> )	UAS-tII	Kyoto DGRC	109680	
Genetic reagent ( <i>D. melanogaster</i> )	UAS-tII-miRNA[s]	(Lin et al., 2009)		
Genetic reagent ( <i>D. melanogaster</i> )	UAS-tII-shRNA	VDRC	330031	
Genetic reagent ( <i>D. melanogaster</i> )	UAS-TLX	this study		Human TLX under the control of UAS
Genetic reagent ( <i>D. melanogaster</i> )	G-TRACE	BDSC	RRID:BDSC_28280	
Genetic reagent ( <i>D. melanogaster</i> )	G-TRACE	BDSC	RRID:BDSC_28281	
Genetic reagent ( <i>D. melanogaster</i> )	erm-CD4-tdTomato	(Han et al., 2011)		R9D11-CD4-tdTomato
Genetic reagent ( <i>D. melanogaster</i> )	erm-mCD8-GFP	(Zhu et al., 2011)		R9D11-mCD8-GFP
Genetic reagent ( <i>D. melanogaster</i> )	erm-lacZ	(Haenfler et al., 2012)		R9D11-lacZ
Genetic reagent ( <i>D. melanogaster</i> )	TII-GFP	BDSC	RRID:BDSC_30874	

Continued on next page

Continued

Reagent type (species) or resource	Designation	Source or reference	Identifiers	Additional information
Genetic reagent ( <i>D. melanogaster</i> )	Pnt-GFP	BDSC	RRID:BDSC_42680	
Genetic reagent ( <i>D. melanogaster</i> )	FRT82B, <i>tub</i> -GAL80	BDSC	RRID:BDSC_5135	
Genetic reagent ( <i>D. melanogaster</i> )	FRT82B	BDSC	RRID:BDSC_2035	
Genetic reagent ( <i>D. melanogaster</i> )	FRT82B, <i>tll</i> <sup>149</sup> /TM6B	(Pignoni et al., 1990)		
Genetic reagent ( <i>D. melanogaster</i> )	dpn>KDRTs-stop-KDRTs>GAL4	(Yang et al., 2016)		
Genetic reagent ( <i>D. melanogaster</i> )	ase-GAL80	(Neumüller et al., 2011)		
Genetic reagent ( <i>D. melanogaster</i> )	stg14- <i>kd</i>	(Yang et al., 2016)		
Antibody	rabbit anti-Ase (polyclonal)	(Brand et al., 1993) Gift from the Jan Lab		IF 1:2,000
Antibody	chicken anti-β-Galactosidase (polyclonal)	abcam	ab9361	IF 1:1,000
Antibody	rabbit anti-β-Galactosidase (polyclonal)	Cappel (now MP Biomedicals)	55976	IF 1:10,000
Antibody	guinea pig anti-Dpn (polyclonal)	(Caygill and Brand, 2017)		IF 1:5,000
Antibody	rat anti-Elav (monoclonal)	DSHB	7E8A10 conc.	IF 1:100
Antibody	chicken anti-GFP (polyclonal)	abcam	ab13970	IF 1:2,000
Antibody	rabbit anti-PntP1 (polyclonal)	A gift from Jim Skeath		IF 1:500
Antibody	mouse anti-Pros (monoclonal)	DSHB	MR1A	IF 1:30
Antibody	rabbit anti-Tll (polyclonal)	(Kosman et al., 1998) Asian Distribution Center for Segmentation Antibodies		IF 1:300

## Fly stocks and husbandry

*Drosophila melanogaster* were reared in cages at 25 °C. Embryos were collected on yeasted apple juice plates. For experiments involving GAL80<sup>ts</sup> embryos were kept at 18 °C until hatching. After hatching, larvae were transferred to a yeasted food plate and reared to the desired stage before dissection. Please see **Supplementary file 1** for experimental genotypes and the temperature at which larvae were raised for each experiment.

The following GAL4 lines were used: Ay-GAL4, UAS-GFP (BL4411), Ay-GAL4, UAS-*lacZ*(*nls*) (BL4410), *btd*-GAL4 (Estella et al., 2003), *erm*-GAL4 (Pfeiffer et al., 2008; Weng et al., 2010) (R9D11-GAL4, BL40731), GMR71C09-GAL4 (Li et al., 2014) (BL39575), *insc*-GAL4 (GAL4<sup>MZ1407</sup>) (Luo et al., 1994), *pntP1*<sup>14-94</sup>-GAL4 (Zhu et al., 2011), *wor*-GAL4 (Albertson et al., 2004), OK371-GAL4 (VGlut<sup>OK371</sup>-GAL4) (BL26160). *tub*-GAL80<sup>ts</sup> (BL7018) was used to restrict GAL4 activity to larval stages as indicated.

The following UAS-transgenes were used: UAS-*ase* (Brand et al., 1993), UAS-*FLP* (BL4539 and BL4540), UAS-*lacZ* (Brand and Perrimon, 1993), UAS-*LT3-NDam* (Southall et al., 2013) and UAS-*LT3-NDam-tll* (this study), UAS-*mCD8-GFP* (BL5130 and BL5137), UAS-*mCD8-mCherry* (BL27391), UAS-*myr-mRFP* (BL7118 and BL7119), UAS-*tll* (Kurusu et al., 2009) (Kyoto Stock Center 109680),

UAS-*tll*-miRNA[s] (Lin et al., 2009), UAS-*tll*-shRNA (VDRC 330031), UAS-TLX (this study), G-TRACE (BL28280 and BL28281). *w*<sup>1118</sup> was used as a reference stock.

The following reporter lines were used: *erm*-CD4-tdTomato (R9D11-CD4-tdTomato) (Han et al., 2011), *erm*-mCD8-GFP (R9D11-mCD8-GFP) (Zhu et al., 2011), *erm*-*lacZ* (R9D11-*lacZ*) (Haenfler et al., 2012) and TII-GFP (Venken et al., 2009) (BL30874). TII-GFP is a protein fusion under the control of a 20 kb insert containing the *tll* coding sequence and surrounding regulatory sequences. Importantly, this construct can rescue the lethality of homozygous *tll*<sup>49</sup> mutants (data not shown). Pnt-GFP (BL42680) is a protein fusion under the control of a 90.7 kb insert containing the *pnt* coding sequence and surrounding regulatory sequences. This construct can rescue the lethality of *pnt* amorphic heteroallelic combinations (Boisclair Lachance et al., 2014).

For MARCM clone analysis, virgin female flies carrying *hsFLP*<sup>122</sup>; *wor*-GAL4, UAS-*mCD8-mCherry*/(CyOact-GFP); FRT82B, *tub*-GAL80 were crossed to male flies carrying *w*; *erm-lacZ*; FRT82B or *w*; *erm-lacZ*; FRT82B, *tll*<sup>49</sup>/TM6B. *tll*<sup>49</sup> is strong *tll* point mutation that is homozygous embryonic lethal (Pignoni et al., 1990). Embryos were collected on apple juice plates at 25°C and newly hatched larvae were transferred to yeast food plates and raised at 25°C. Clones were induced by a heat shock in a water bath (5 min 37°C, 5 min rest at room temperature, 1 hr 37°C) at 24 hr ALH and larvae were dissected 72 hr later.

## Immunostaining

Brains were dissected in PBS, fixed in 4% formaldehyde/PBS for 20 min at room temperature and washed with PBS with 0.3% TritonX-100 (PBTx). Samples were blocked with 10% normal goat serum before overnight incubation with the following antisera: rabbit anti-Ase 1:2,000 (Brand et al., 1993) (a gift from the Jan lab), chicken anti-β-Galactosidase 1:1,000 (abcam ab9361), rabbit anti-β-Galactosidase 1:10,000 (Cappel), guinea pig anti-Dpn 1:5,000 (Caygill and Brand, 2017), rat anti-Elav 1:100 (DSHB, 7E8A10 conc.), chicken anti-GFP 1:2,000 (abcam ab13970), rabbit anti-PntP1 (1:500) (a gift from the Jim Skeath), mouse anti-Pros 1:30 (DSHB, MR1A), rabbit anti-TII 1:300 (Kosman et al., 1998). Secondary antibodies conjugated to Alexa-405, Alexa-488, Alexa-546, Alexa-568, Alexa-633 all 1:500 (Life Technologies) or DyLight-405 1:200 (Jackson Laboratories) were used. Samples were mounted in Vectashield (Vector Laboratories) for imaging.

## *tll* RNA FISH

A set of 38 Stellaris FISH probes was designed against the *tll* coding sequence and labeled with Quasar 570. Third instar larval brains were fixed in 4% formaldehyde/PBS for 45 min at room temperature and then permeabilized in 70% ethanol/PBS for 6 hr at 4 °C. Brains were washed with Wash Buffer (10% formamide, 2xSSC) for 5 min before being incubated with probes (125 nM) in hybridisation buffer (100 mg/mL dextran sulfate, 10% formamide, 2xSSC) overnight at 45 °C. Brains were washed with Wash Buffer, stained with DAPI and mounted in Vectashield (Vector Laboratories) for imaging.

## Image acquisition and processing

Fluorescent images were acquired using a Leica SP8 confocal microscope. Images were analysed using Fiji (Schindelin et al., 2012), which was also used to adjust brightness and contrast in images. Adobe Illustrator was used to compile figures.

## Quantification and statistical analysis

GraphPad Prism version 7.00 for Mac OS X ([www.graphpad.com](http://www.graphpad.com)) was used for statistical analysis. No data were excluded.

## Sequence alignment of human TLX and *Drosophila* TII

Sequence alignment performed using EMBOSS Needle ([https://www.ebi.ac.uk/Tools/psa/emboss\\_needle/](https://www.ebi.ac.uk/Tools/psa/emboss_needle/)) and UniProt alignment (<https://www.uniprot.org/align/>) tools.

## Generation of UAS-TLX

The coding sequence of human TLX (Jackson et al., 1998) was amplified from cDNA prepared from H9 ESCs (a kind gift from T. Otani) using the primers fwd: 5'-AGATGAATTCA

TGAGCAAGCCAGCCGG-3' and rev: 5'-ATGACTCGAGTTAGATATCACTGGATTTGTACATATC TGAAAGCAGTC-3'. The amplified product was cloned (using restriction enzymes EcoR1 and XhoI) into pUAST-attB and then integrated into attP40 by standard methods.

### Generation of UAS-LT3-NDam-*tII*

The coding sequence of *tII* was amplified from an embryonic cDNA library using the primers fwd: 5'-cagaaactcatctctgaagaggatctgagatctaATGCAGTCGTCGGAGG-3' and rev: 5' acagaagtaaggttccttcacaaagatcctctagaTCAGATCTTGCGCTGACT 3'. The amplified product was cloned via Gibson assembly into pUASTattB-LT3-NDam (Southall et al., 2013) cut with BglII and XbaI and then integrated into attP40 by standard methods.

### Targeted DamID

We used a recombinase-dependent system to restrict GAL4 expression to Type II lineages (Yang et al., 2016). *dpn* >KDRTs-stop-KDRTs>GAL4; *ase*-GAL80/CyOact-GFP; + virgins were crossed to *w*; UAS-LT3-NDam-*tII*; *stg14-kd* or *w*; UAS-LT3-NDam; *stg14-kd* males at 25 °C. Larvae were transferred to yeasted food plates within an hour of hatching and dissected 50 hr later. Analysis was performed using the damidseq\_pipeline as described previously (Marshall et al., 2016). *dpn* >KDRTs-stop-KDRTs>GAL4 and *stg14-kd* flies were provided by T. Lee (Yang et al., 2016) and *ase*-GAL80 flies by J. Knoblich (Neumüller et al., 2011). DamID analysis was performed as described previously (Marshall and Brand, 2015) and the Integrative Genomics Viewer (IGV, version 2.3.68) was used to visualise binding tracks aligned to release 6 of the *Drosophila* genome.

### RNA single cell sequencing analysis

Single cell sequencing analysis was performed using Seurat version 3. Data was obtained from Neftel et al. (2019), which was made available through the Broad Institute Single-Cell Portal ([https://portals.broadinstitute.org/single\\_cell/study/SCP393/single-cell-rna-seq-of-adult-and-pediatric-glioblastoma](https://portals.broadinstitute.org/single_cell/study/SCP393/single-cell-rna-seq-of-adult-and-pediatric-glioblastoma)) and the Gene Expression Omnibus (GEO: GSE131928).

### Acknowledgements

We should like to thank L Jan and Y N Jan, J Knoblich, M Kurusu, C-Y. Lee, T Lee, T Otani, J Skeath, S Zhu, the Asian Distribution Centre for Segmentation Antibodies, Bloomington *Drosophila* Stock Centre, Developmental Studies Hybridoma Bank (DSHB), the Kyoto Stock Center (DGRC), and the Vienna *Drosophila* Resource Center (VDRC) for reagents. We thank D J Kunz for advice on glioblastoma single cell RNA sequencing data, LYJ Tang for performing single cell RNA sequencing analysis and R Krautz for analyzing the TII TaDa binding data. We thank L Otsuki for helpful discussions.

This work was funded by Wellcome Trust Senior Investigator Award (103792 to AHB) and the Royal Society Darwin Trust Research Professorship (to AHB) and Wellcome Trust PhD Studentship (102454 to AEH). AHB acknowledges core funding to The Gurdon Institute from the Wellcome Trust (092096) and CRUK (C6946/A14492).

### Additional information

#### Funding

Funder	Grant reference number	Author
Wellcome	103792	Andrea H Brand
Royal Society		Andrea H Brand
Wellcome	102454	Anna E Hakes
Wellcome	092096	Andrea H Brand
Cancer Research UK	C6946/A14492	Andrea H Brand

The funders had no role in study design, data collection and interpretation, or the decision to submit the work for publication.



### Author contributions

Anna E Hakes, Conceptualization, Resources, Data curation, Formal analysis, Investigation, Methodology; Andrea H Brand, Conceptualization, Resources, Formal analysis, Supervision, Funding acquisition, Investigation, Project administration

### Author ORCIDs

Anna E Hakes  <https://orcid.org/0000-0002-8664-1014>

Andrea H Brand  <https://orcid.org/0000-0002-2089-6954>

### Decision letter and Author response

Decision letter <https://doi.org/10.7554/eLife.53377.sa1>

Author response <https://doi.org/10.7554/eLife.53377.sa2>

## Additional files

### Supplementary files

- Supplementary file 1. *Drosophila* genotypes and experimental conditions.
- Transparent reporting form

### Data availability

All data generated or analysed during this study are included in the manuscript and supporting files.

The following previously published dataset was used:

Author(s)	Year	Dataset title	Dataset URL	Database and Identifier
Neftel C, Laffy J, Filbin MG, Hara T	2019	single cell RNA-seq analysis of adult and paediatric IDH-wildtype Glioblastomas	<a href="https://www.ncbi.nlm.nih.gov/geo/query/acc.cgi?acc=GSE131928">https://www.ncbi.nlm.nih.gov/geo/query/acc.cgi?acc=GSE131928</a>	NCBI Gene Expression Omnibus, GSE131928

## References

- Albertson R, Chabu C, Sheehan A, Doe CQ. 2004. Scribble protein domain mapping reveals a multistep localization mechanism and domains necessary for establishing cortical polarity. *Journal of Cell Science* **117**: 6061–6070. DOI: <https://doi.org/10.1242/jcs.01525>, PMID: 15536119
- Alcantara Llaguno S, Chen J, Kwon CH, Jackson EL, Li Y, Burns DK, Alvarez-Buylla A, Parada LF. 2009. Malignant astrocytomas originate from neural stem/progenitor cells in a somatic tumor suppressor mouse model. *Cancer Cell* **15**:45–56. DOI: <https://doi.org/10.1016/j.ccr.2008.12.006>, PMID: 19111880
- Alcantara Llaguno SR, Wang Z, Sun D, Chen J, Xu J, Kim E, Hatanpaa KJ, Raisanen JM, Burns DK, Johnson JE, Parada LF. 2015. Adult Lineage-Restricted CNS progenitors specify distinct glioblastoma subtypes. *Cancer Cell* **28**:429–440. DOI: <https://doi.org/10.1016/j.ccell.2015.09.007>, PMID: 26461091
- Alcantara Llaguno S, Sun D, Pedraza AM, Vera E, Wang Z, Burns DK, Parada LF. 2019. Cell-of-origin susceptibility to glioblastoma formation declines with neural lineage restriction. *Nature Neuroscience* **22**:545–555. DOI: <https://doi.org/10.1038/s41593-018-0333-8>, PMID: 30778149
- Bachoo RM, Maher EA, Ligon KL, Sharpless NE, Chan SS, You MJ, Tang Y, DeFrances J, Stover E, Weissleder R, Rowitch DH, Louis DN, DePinho RA. 2002. Epidermal growth factor receptor and *Ink4a/Arf*: convergent mechanisms governing terminal differentiation and transformation along the neural stem cell to astrocyte Axis. *Cancer Cell* **1**:269–277. DOI: [https://doi.org/10.1016/s1535-6108\(02\)00046-6](https://doi.org/10.1016/s1535-6108(02)00046-6), PMID: 12086863
- Bayraktar OA, Boone JQ, Drummond ML, Doe CQ. 2010. *Drosophila* type II neuroblast lineages keep Prospero levels low to generate large clones that contribute to the adult brain central complex. *Neural Development* **5**: 26. DOI: <https://doi.org/10.1186/1749-8104-5-26>, PMID: 20920301
- Bello BC, Izergina N, Caussinus E, Reichert H. 2008. Amplification of neural stem cell proliferation by intermediate progenitor cells in *Drosophila* brain development. *Neural Development* **3**:5. DOI: <https://doi.org/10.1186/1749-8104-3-5>
- Bier E, Vaessin H, Younger-Shepherd S, Jan LY, Jan YN. 1992. *Deadpan*, an essential pan-neural gene in *Drosophila*, encodes a helix-loop-helix protein similar to the *hairy* gene product. *Genes & Development* **6**: 2137–2151. DOI: <https://doi.org/10.1101/gad.6.11.2137>
- Boisclair Lachance JF, Peláez N, Cassidy JJ, Webber JL, Rebay I, Carthew RW. 2014. A comparative study of pointed and yan expression reveals new complexity to the transcriptional networks downstream of receptor

- tyrosine kinase signaling. *Developmental Biology* **385**:263–278. DOI: <https://doi.org/10.1016/j.ydbio.2013.11.002>, PMID: 24240101
- Boone JQ, Doe CQ. 2008. Identification of *Drosophila* type II neuroblast lineages containing transit amplifying ganglion mother cells. *Developmental Neurobiology* **68**:1185–1195. DOI: <https://doi.org/10.1002/dneu.20648>, PMID: 18548484
- Bowman SK, Rolland V, Betschinger J, Kinsey KA, Emery G, Knoblich JA. 2008. The tumor suppressors brat and numb regulate transit-amplifying neuroblast lineages in *Drosophila*. *Developmental Cell* **14**:535–546. DOI: <https://doi.org/10.1016/j.devcel.2008.03.004>, PMID: 18342578
- Brand M, Jarman AP, Jan LY, Jan YN. 1993. Asense is a *Drosophila* neural precursor gene and is capable of initiating sense organ formation. *Development* **119**:1–17. PMID: 8565817
- Brand AH, Perrimon N. 1993. Targeted gene expression as a means of altering cell fates and generating dominant phenotypes. *Development* **118**:401–415. PMID: 8223268
- Cabernard C, Doe CQ. 2009. Apical/basal spindle orientation is required for neuroblast homeostasis and neuronal differentiation in *Drosophila*. *Dev Cell* **17**:134–141. DOI: <https://doi.org/10.1016/j.devcel.2009.06.009>
- Caygill EE, Brand AH. 2017. miR-7 buffers differentiation in the developing *Drosophila* Visual System. *Cell Reports* **20**:1255–1261. DOI: <https://doi.org/10.1016/j.celrep.2017.07.047>, PMID: 28793250
- Chen J, Kwon CH, Lin L, Li Y, Parada LF. 2009. Inducible site-specific recombination in neural stem/progenitor cells. *Genesis* **47**:122–131. DOI: <https://doi.org/10.1002/dvg.20465>, PMID: 19117051
- Chen X, Wanggou S, Bodalia A, Zhu M, Dong W, Fan JJ, Yin WC, Min HK, Hu M, Draghici D, Dou W, Li F, Coutinho FJ, Whetstone H, Kushida MM, Dirks PB, Song Y, Hui CC, Sun Y, Wang LY, et al. 2018. A feedforward mechanism mediated by mechanosensitive ion channel PIEZO1 and tissue mechanics promotes glioma aggression. *Neuron* **100**:799–815. DOI: <https://doi.org/10.1016/j.neuron.2018.09.046>, PMID: 30344046
- Chen AS, Wardwell-Ozgo J, Shah NN, Wright D, Appin CL, Vigneswaran K, Brat DJ, Kornblum HI, Read RD. 2019. Drak/STK17A drives neoplastic glial proliferation through modulation of MRLC signaling. *Cancer Research* **79**:1085–1097. DOI: <https://doi.org/10.1158/0008-5472.CAN-18-0482>, PMID: 30530503
- Chen AS, Read RD. 2019. *Drosophila melanogaster* as a model system for human glioblastomas. *Advances in Experimental Medicine and Biology* **1167**:207–224. DOI: [https://doi.org/10.1007/978-3-030-23629-8\\_12](https://doi.org/10.1007/978-3-030-23629-8_12), PMID: 31520357
- Chow LM, Endersby R, Zhu X, Rankin S, Qu C, Zhang J, Broniscer A, Ellison DW, Baker SJ. 2011. Cooperativity within and among pten, p53, and rb pathways induces high-grade astrocytoma in adult brain. *Cancer Cell* **19**:305–316. DOI: <https://doi.org/10.1016/j.ccr.2011.01.039>, PMID: 21397855
- Curt JR, Yaghmaeian Salmani B, Thor S. 2019. Anterior CNS expansion driven by brain transcription factors. *eLife* **8**:e45274. DOI: <https://doi.org/10.7554/eLife.45274>, PMID: 31271353
- Deng W-M. 2019. *The Drosophila Model in Cancer*. Cham: Springer International Publishing. DOI: <https://doi.org/10.1007/978-3-030-23629-8>
- Diaz RJ, Harbecke R, Singer JB, Pignoni F, Janning W, Lengyel JA. 1996. Graded effect of *tailless* on posterior gut development: molecular basis of an allelic series of a nuclear receptor gene. *Mechanisms of Development* **54**:119–130. DOI: [https://doi.org/10.1016/0925-4773\(95\)00467-X](https://doi.org/10.1016/0925-4773(95)00467-X), PMID: 8808411
- Doetsch F, Caillé I, Lim DA, Garcia-Verdugo JM, Alvarez-Buylla A. 1999. Subventricular zone astrocytes are neural stem cells in the adult mammalian brain. *Cell* **97**:703–716. DOI: [https://doi.org/10.1016/S0092-8674\(00\)80783-7](https://doi.org/10.1016/S0092-8674(00)80783-7), PMID: 10380923
- Elsir T, Eriksson A, Orrego A, Lindström MS, Nistér M. 2010. Expression of PROX1 is a common feature of high-grade malignant astrocytic gliomas. *Journal of Neuropathology & Experimental Neurology* **69**:129–138. DOI: <https://doi.org/10.1097/NEN.0b013e3181ca4767>, PMID: 20084020
- Estella C, Rieckhof G, Calleja M, Morata G. 2003. The role of buttonhead and Sp1 in the development of the ventral imaginal discs of *Drosophila*. *Development* **130**:5929–5941. DOI: <https://doi.org/10.1242/dev.00832>, PMID: 14561634
- Evans CJ, Olson JM, Ngo KT, Kim E, Lee NE, Kuoy E, Patananan AN, Sitz D, Tran P, Do MT, Yackle K, Cespedes A, Hartenstein V, Call GB, Banerjee U. 2009. G-TRACE: rapid Gal4-based cell lineage analysis in *Drosophila*. *Nature Methods* **6**:603–605. DOI: <https://doi.org/10.1038/nmeth.1356>, PMID: 19633663
- Friedmann-Morvinski D, Bushong EA, Ke E, Soda Y, Marumoto T, Singer O, Ellisman MH, Verma IM. 2012. Dedifferentiation of neurons and astrocytes by oncogenes can induce gliomas in mice. *Science* **338**:1080–1084. DOI: <https://doi.org/10.1126/science.1226929>, PMID: 23087000
- Goudarzi KM, Espinoza JA, Guo M, Bartek J, Nistér M, Lindström MS, Hägerstrand D. 2018. Reduced expression of PROX1 transitions glioblastoma cells into a mesenchymal gene expression subtype. *Cancer Research* **78**:5901–5916. DOI: <https://doi.org/10.1158/0008-5472.CAN-18-0320>, PMID: 30135192
- Haeflner JM, Kuang C, Lee CY. 2012. Cortical aPKC kinase activity distinguishes neural stem cells from progenitor cells by ensuring asymmetric segregation of numb. *Developmental Biology* **365**:219–228. DOI: <https://doi.org/10.1016/j.ydbio.2012.02.027>, PMID: 22394487
- Hakes AE, Brand AH. 2019. Neural stem cell dynamics: the development of brain tumours. *Current Opinion in Cell Biology* **60**:131–138. DOI: <https://doi.org/10.1016/j.ceb.2019.06.001>, PMID: 31330360
- Han C, Jan LY, Jan YN. 2011. Enhancer-driven membrane markers for analysis of nonautonomous mechanisms reveal neuron-glia interactions in *Drosophila*. *PNAS* **108**:9673–9678. DOI: <https://doi.org/10.1073/pnas.1106386108>, PMID: 21606367
- Harding K, White K. 2018. *Drosophila* as a model for developmental biology: stem Cell-Fate decisions in the developing nervous system. *Journal of Developmental Biology* **6**:25. DOI: <https://doi.org/10.3390/jdb6040025>

- Holland EC**, Celestino J, Dai C, Schaefer L, Sawaya RE, Fuller GN. 2000. Combined activation of ras and akt in neural progenitors induces glioblastoma formation in mice. *Nature Genetics* **25**:55–57. DOI: <https://doi.org/10.1038/75596>, PMID: 10802656
- Ito K**, Awano W, Suzuki K, Hiromi Y, Yamamoto D. 1997. The *Drosophila* mushroom body is a quadruple structure of clonal units each of which contains a virtually identical set of neurones and glial cells. *Development* **124**:761–771. PMID: 9043058
- Jackson A**, Panayiotidis P, Foroni L. 1998. The human homologue of the *Drosophila* tailless gene (TLX): characterization and mapping to a region of common deletion in human lymphoid leukemia on chromosome 6q21. *Genomics* **50**:34–43. DOI: <https://doi.org/10.1006/geno.1998.5270>, PMID: 9628820
- Kim EJ**, Ables JL, Dickel LK, Eisch AJ, Johnson JE. 2011. Ascl1 (Mash1) defines cells with long-term neurogenic potential in Subgranular and subventricular zones in adult mouse brain. *PLOS ONE* **6**:e18472. DOI: <https://doi.org/10.1371/journal.pone.0018472>, PMID: 21483754
- Kosman D**, Small S, Reinitz J. 1998. Rapid preparation of a panel of polyclonal antibodies to *Drosophila* segmentation proteins. *Development Genes and Evolution* **208**:290–294. DOI: <https://doi.org/10.1007/s004270050184>, PMID: 9683745
- Kurusu M**, Maruyama Y, Adachi Y, Okabe M, Suzuki E, Furukubo-Tokunaga K. 2009. A conserved nuclear receptor, tailless, is required for efficient proliferation and prolonged maintenance of mushroom body progenitors in the *Drosophila* brain. *Developmental Biology* **326**:224–236. DOI: <https://doi.org/10.1016/j.ydbio.2008.11.013>, PMID: 19084514
- Lee JH**, Lee JE, Kahng JY, Kim SH, Park JS, Yoon SJ, Um JY, Kim WK, Lee JK, Park J, Kim EH, Lee JH, Lee JH, Chung WS, Ju YS, Park SH, Chang JH, Kang SG, Lee JH. 2018. Human glioblastoma arises from subventricular zone cells with low-level driver mutations. *Nature* **560**:243–247. DOI: <https://doi.org/10.1038/s41586-018-0389-3>, PMID: 30069053
- Lee T**, Luo L. 1999. Mosaic analysis with a repressible cell marker for studies of gene function in neuronal morphogenesis. *Neuron* **22**:451–461. DOI: [https://doi.org/10.1016/S0896-6273\(00\)80701-1](https://doi.org/10.1016/S0896-6273(00)80701-1), PMID: 10197526
- Li W**, Sun G, Yang S, Qu Q, Nakashima K, Shi Y. 2008. Nuclear receptor TLX regulates cell cycle progression in neural stem cells of the developing brain. *Molecular Endocrinology* **22**:56–64. DOI: <https://doi.org/10.1210/me.2007-0290>, PMID: 17901127
- Li S**, Sun G, Murai K, Ye P, Shi Y. 2012. Characterization of TLX expression in neural stem cells and progenitor cells in adult brains. *PLOS ONE* **7**:e43324. DOI: <https://doi.org/10.1371/journal.pone.0043324>, PMID: 22952666
- Li HH**, Kroll JR, Lennox SM, Ogundeyi O, Jeter J, Depasquale G, Truman JW. 2014. A GAL4 driver resource for developmental and behavioral studies on the larval CNS of *Drosophila*. *Cell Reports* **8**:897–908. DOI: <https://doi.org/10.1016/j.celrep.2014.06.065>, PMID: 25088417
- Lin S**, Huang Y, Lee T. 2009. Nuclear receptor unfulfilled regulates axonal guidance and cell identity of *Drosophila* mushroom body neurons. *PLOS ONE* **4**:e8392. DOI: <https://doi.org/10.1371/journal.pone.0008392>, PMID: 20027309
- Lindberg N**, Kastemar M, Olofsson T, Smits A, Uhrbom L. 2009. Oligodendrocyte progenitor cells can act as cell of origin for experimental glioma. *Oncogene* **28**:2266–2275. DOI: <https://doi.org/10.1038/onc.2009.76>, PMID: 19421151
- Liu HK**, Belz T, Bock D, Takacs A, Wu H, Lichter P, Chai M, Schütz G. 2008. The nuclear receptor tailless is required for neurogenesis in the adult subventricular zone. *Genes & Development* **22**:2473–2478. DOI: <https://doi.org/10.1101/gad.479308>, PMID: 18794344
- Liu HK**, Wang Y, Belz T, Bock D, Takacs A, Radlwimmer B, Barbus S, Reifenberger G, Lichter P, Schütz G. 2010. The nuclear receptor tailless induces long-term neural stem cell expansion and brain tumor initiation. *Genes & Development* **24**:683–695. DOI: <https://doi.org/10.1101/gad.560310>, PMID: 20360385
- Luo L**, Liao YJ, Jan LY, Jan YN. 1994. Distinct morphogenetic functions of similar small GTPases: *Drosophila* Drac1 is involved in axonal outgrowth and myoblast fusion. *Genes & Development* **8**:1787–1802. DOI: <https://doi.org/10.1101/gad.8.15.1787>
- Marshall OJ**, Southall TD, Cheetham SW, Brand AH. 2016. Cell-type-specific profiling of protein-DNA interactions without cell isolation using targeted DamID with next-generation sequencing. *Nature Protocols* **11**:1586–1598. DOI: <https://doi.org/10.1038/nprot.2016.084>, PMID: 27490632
- Marshall OJ**, Brand AH. 2015. damidseq\_pipeline: an automated pipeline for processing DamID sequencing datasets: Fig. 1. *Bioinformatics* **31**:3371–3373. DOI: <https://doi.org/10.1093/bioinformatics/btv386>
- Marumoto T**, Tashiro A, Friedmann-Morvinski D, Scadeng M, Soda Y, Gage FH, Verma IM. 2009. Development of a novel mouse glioma model using lentiviral vectors. *Nature Medicine* **15**:110–116. DOI: <https://doi.org/10.1038/nm.1863>, PMID: 19122659
- Neftel C**, Laffy J, Filbin MG, Hara T, Shore ME, Rahme GJ, Richman AR, Silverbush D, Shaw ML, Hebert CM, Dewitt J, Gritsch S, Perez EM, Gonzalez Castro LN, Lan X, Druck N, Rodman C, Dionne D, Kaplan A, Bertalan MS, et al. 2019. An integrative model of cellular states, plasticity, and genetics for glioblastoma. *Cell* **178**:835–849. DOI: <https://doi.org/10.1016/j.cell.2019.06.024>, PMID: 31327527
- Neumüller RA**, Richter C, Fischer A, Novatchkova M, Neumüller KG, Knoblich JA. 2011. Genome-wide analysis of self-renewal in *Drosophila* neural stem cells by transgenic RNAi. *Cell Stem Cell* **8**:580–593. DOI: <https://doi.org/10.1016/j.stem.2011.02.022>, PMID: 21549331
- Niu W**, Zou Y, Shen C, Zhang CL. 2011. Activation of postnatal neural stem cells requires nuclear receptor TLX. *Journal of Neuroscience* **31**:13816–13828. DOI: <https://doi.org/10.1523/JNEUROSCI.1038-11.2011>, PMID: 21957244

- Obernier K**, Simeonova I, Fila T, Mandl C, Hölzl-Wenig G, Monaghan-Nichols P, Ciccolini F. 2011. Expression of *tlx* in Both Stem Cells and Transit Amplifying Progenitors Regulates Stem Cell Activation and Differentiation in the Neonatal Lateral Subependymal Zone. *Stem Cells* **29**:1415–1426. DOI: <https://doi.org/10.1002/stem.682>, PMID: 21714038
- Park HJ**, Kim JK, Jeon HM, Oh SY, Kim SH, Nam DH, Kim H. 2010. The neural stem cell fate determinant TLX promotes tumorigenesis and genesis of cells resembling glioma stem cells. *Molecules and Cells* **30**:403–408. DOI: <https://doi.org/10.1007/s10059-010-0122-z>, PMID: 20814749
- Park NI**, Guilhamon P, Desai K, McAdam RF, Langille E, O'Connor M, Lan X, Whetstone H, Coutinho FJ, Vanner RJ, Ling E, Prinos P, Lee L, Selvadurai H, Atwal G, Kushida M, Clarke ID, Voisin V, Cusimano MD, Bernstein M, et al. 2017. ASCL1 reorganizes chromatin to direct neuronal fate and suppress tumorigenicity of glioblastoma stem cells. *Cell Stem Cell* **21**:411. DOI: <https://doi.org/10.1016/j.stem.2017.08.008>, PMID: 28886368
- Parras CM**, Galli R, Britz O, Soares S, Galichet C, Battiste J, Johnson JE, Nakafuku M, Vescovi A, Guillemot F. 2004. *Mash1* specifies neurons and oligodendrocytes in the postnatal brain. *The EMBO Journal* **23**:4495–4505. DOI: <https://doi.org/10.1038/sj.emboj.7600447>, PMID: 15496983
- Pfeiffer BD**, Jenett A, Hammonds AS, Ngo TT, Misra S, Murphy C, Scully A, Carlson JW, Wan KH, Lavery TR, Mungall C, Svirskas R, Kardon JT, Doe CQ, Eisen MB, Celniker SE, Rubin GM. 2008. Tools for neuroanatomy and neurogenetics in *Drosophila*. *PNAS* **105**:9715–9720. DOI: <https://doi.org/10.1073/pnas.0803697105>, PMID: 18621688
- Pignoni F**, Baldarelli RM, Steingrímsson E, Diaz RJ, Patapoutian A, Merriam JR, Lengyel JA. 1990. The *Drosophila* gene *tailless* is expressed at the embryonic termini and is a member of the steroid receptor superfamily. *Cell* **62**:151–163. DOI: [https://doi.org/10.1016/0092-8674\(90\)90249-E](https://doi.org/10.1016/0092-8674(90)90249-E), PMID: 2364433
- Ramon-Cañellas P**, Peterson HP, Morante J. 2019. From early to late neurogenesis: neural progenitors and the glial niche from a fly's Point of View. *Neuroscience* **399**:39–52. DOI: <https://doi.org/10.1016/j.neuroscience.2018.12.014>
- Read RD**, Cavenee WK, Furnari FB, Thomas JB. 2009. A *Drosophila* Model for EGFR-Ras and PI3K-Dependent Human Glioma. *PLOS Genetics* **5**:e1000374. DOI: <https://doi.org/10.1371/journal.pgen.1000374>
- Read RD**, Fenton TR, Gomez GG, Wykosky J, Vandenberg SR, Babic I, Iwanami A, Yang H, Cavenee WK, Mischel PS, Furnari FB, Thomas JB. 2013. A kinome-wide RNAi screen in *Drosophila* Glia reveals that the RIO kinases mediate cell proliferation and survival through TORC2-Akt signaling in glioblastoma. *PLOS Genetics* **9**:e1003253. DOI: <https://doi.org/10.1371/journal.pgen.1003253>, PMID: 23459592
- Roodakker KR**, Elsir T, Edqvist PD, Hägerstrand D, Carlson J, Lysiak M, Henriksson R, Pontén F, Rosell J, Söderkvist P, Stupp R, Tchougounova E, Nistér M, Malmström A, Smits A. 2016. PROX1 is a novel pathway-specific prognostic biomarker for high-grade astrocytomas; results from independent glioblastoma cohorts stratified by age and IDH mutation status. *Oncotarget* **7**:72431–72442. DOI: <https://doi.org/10.18632/oncotarget.11957>, PMID: 27626492
- Schindelin J**, Arganda-Carreras I, Frise E, Kaynig V, Longair M, Pietzsch T, Preibisch S, Rueden C, Saalfeld S, Schmid B, Tinevez JY, White DJ, Hartenstein V, Eliceiri K, Tomancak P, Cardona A. 2012. Fiji: an open-source platform for biological-image analysis. *Nature Methods* **9**:676–682. DOI: <https://doi.org/10.1038/nmeth.2019>, PMID: 22743772
- Shi Y**, Chichung Lie D, Taupin P, Nakashima K, Ray J, Yu RT, Gage FH, Evans RM. 2004. Expression and function of orphan nuclear receptor TLX in adult neural stem cells. *Nature* **427**:78–83. DOI: <https://doi.org/10.1038/nature02211>, PMID: 14702088
- Southall TD**, Gold KS, Egger B, Davidson CM, Caygill EE, Marshall OJ, Brand AH. 2013. Cell-Type-Specific Profiling of Gene Expression and Chromatin Binding without Cell Isolation: Assaying RNA Pol II Occupancy in Neural Stem Cells. *Developmental Cell* **26**:101–112. DOI: <https://doi.org/10.1016/j.devcel.2013.05.020>
- Venken KJ**, Carlson JW, Schulze KL, Pan H, He Y, Spokony R, Wan KH, Koriabine M, de Jong PJ, White KP, Bellen HJ, Hoskins RA. 2009. Versatile P[acman] BAC libraries for transgenesis studies in *Drosophila melanogaster*. *Nature Methods* **6**:431–434. DOI: <https://doi.org/10.1038/nmeth.1331>, PMID: 19465919
- Villegas SN**. 2019. One hundred years of *Drosophila* Cancer research: no longer in solitude. *Disease Models & Mechanisms* **12**:dmm039032. DOI: <https://doi.org/10.1242/dmm.039032>, PMID: 30952627
- Wang L**, Rajan H, Pitman JL, McKeown M, Tsai CC. 2006. Histone deacetylase-associating atrophin proteins are nuclear receptor corepressors. *Genes & Development* **20**:525–530. DOI: <https://doi.org/10.1101/gad.1393506>, PMID: 16481466
- Weng M**, Golden KL, Lee CY. 2010. *dFzef/Earmuff* maintains the restricted developmental potential of intermediate neural progenitors in *Drosophila*. *Developmental Cell* **18**:126–135. DOI: <https://doi.org/10.1016/j.devcel.2009.12.007>, PMID: 20152183
- Witte HT**, Jeibmann A, Klämbt C, Paulus W. 2009. Modeling glioma growth and invasion in *Drosophila melanogaster*. *Neoplasia* **11**:882–888. DOI: <https://doi.org/10.1593/neo.09576>, PMID: 19724682
- Xu X**, Wan X, Wei X. 2017. PROX1 promotes human glioblastoma cell proliferation and invasion via activation of the nuclear factor- $\kappa$ B signaling pathway. *Molecular Medicine Reports* **15**:963–968. DOI: <https://doi.org/10.3892/mmr.2016.6075>, PMID: 28035380
- Yang C-P**, Fu C-C, Sugino K, Liu Z, Ren Q, Liu L-Y, Yao X, Lee LP, Lee T. 2016. Transcriptomes of lineage-specific *Drosophila* neuroblasts profiled by genetic targeting and robotic sorting. *Development* **143**:411–421. DOI: <https://doi.org/10.1242/dev.129163>
- Younossi-Hartenstein A**, Green P, Liaw GJ, Rudolph K, Lengyel J, Hartenstein V. 1997. Control of early neurogenesis of the *Drosophila* brain by the head gap genes *tlx*, *otd*, *ems*, and *btd*. *Developmental Biology* **182**:270–283. DOI: <https://doi.org/10.1006/dbio.1996.8475>, PMID: 9070327



- Yu RT**, McKeown M, Evans RM, Umesono K. 1994. Relationship between *Drosophila* gap gene *tailless* and a vertebrate nuclear receptor *tlx*. *Nature* **370**:375–379. DOI: <https://doi.org/10.1038/370375a0>, PMID: 8047143
- Zhang C-L**, Zou Y, He W, Gage FH, Evans RM. 2008. A role for adult TLX-positive neural stem cells in learning and behaviour. *Nature* **451**:1004–1007. DOI: <https://doi.org/10.1038/nature06562>
- Zhi X**, Zhou XE, He Y, Searose-Xu K, Zhang CL, Tsai CC, Melcher K, Xu HE. 2015. Structural basis for corepressor assembly by the orphan nuclear receptor TLX. *Genes & Development* **29**:440–450. DOI: <https://doi.org/10.1101/gad.254904.114>, PMID: 25691470
- Zhu S**, Barshow S, Wildonger J, Jan LY, Jan YN. 2011. Ets transcription factor pointed promotes the generation of intermediate neural progenitors in *Drosophila* larval brains. *PNAS* **108**:20615–20620. DOI: <https://doi.org/10.1073/pnas.1118595109>, PMID: 22143802
- Zhu Z**, Khan MA, Weiler M, Blaes J, Jestaedt L, Geibert M, Zou P, Gronych J, Bernhardt O, Korshunov A, Bugner V, Lichter P, Radlwimmer B, Heiland S, Bendszus M, Wick W, Liu HK. 2014. Targeting self-renewal in high-grade brain tumors leads to loss of brain tumor stem cells and prolonged survival. *Cell Stem Cell* **15**:185–198. DOI: <https://doi.org/10.1016/j.stem.2014.04.007>, PMID: 24835569
- Zou Y**, Niu W, Qin S, Downes M, Burns DK, Zhang CL. 2012. The nuclear receptor TLX is required for gliomagenesis within the adult neurogenic niche. *Molecular and Cellular Biology* **32**:4811–4820. DOI: <https://doi.org/10.1128/MCB.01122-12>, PMID: 23028043